

Photoemission studies of the interaction of oxygen with GaAs(110)

C. Y. Su, I. Lindau, P. W. Chye, P. R. Skeath, and W. E. Spicer
Electrical Engineering Department, Stanford University, Stanford, California 94305

(Received 17 July 1981)

Room-temperature adsorption of oxygen on cleaved GaAs(110) surfaces has been studied with photoemission measurements using synchrotron radiation ($h\nu=20-120$ eV). Particular effort has been spent to obtain the proper photoemission spectrum that represents the density of valence states (DOVS) of the oxygen bonded to GaAs(110). Simple theoretical interpretation, substantiated with comparison made between the DOVS of O-GaAs(110) and the experimental DOVS's of Ga_2O_3 and As_2O_3 , of the DOVS of O-GaAs(110) is given. This interpretation of the DOVS has led to the proposal of a new adsorption model involving both nonbridging oxygen (As=O) and bridging oxygen (Ga-O-As). Evidence extractable from other measurements for the new model is also discussed. Another form of oxygen which saturates at relatively low oxygen coverage (≤ 0.02 monolayer) has also been observed, and is suggested to adsorb at defect sites of the GaAs(110) in the form of Ga-O-Ga units. The role of oxygen adsorption at defect sites in the initial steps of adsorption, particularly the dissociation of oxygen molecules, is discussed. Such discussion is further substantiated by detailed studies of the oxygen adsorption on sputter-disordered GaAs(110) surfaces. A two-step adsorption process has been found to occur on sputter-disordered surfaces. On either ordered or disordered surfaces, direct formation of Ga_2O_3 by room-temperature exposure to unexcited oxygen is highly unlikely. The formation of As_2O_3 by room-temperature adsorption of oxygen on GaAs(110) is also definitely ruled out by thermal annealing experiments. On the other hand, the results of the thermal annealing experiments are consistent with the existence of the As=O bond.

I. INTRODUCTION

The interaction of oxygen with GaAs(110) surfaces has attracted much attention in the past few years.¹⁻⁹ In particular, these studies have addressed the question of adsorption sites and the question of whether oxygen adsorbs nondissociatively or dissociatively.

Several different experimental techniques have been applied to this problem. Among them, the studies of chemical shifts in the Ga $3d$ and in the As $3d$ were often used in the past to address the question of chemisorption sites.^{2,3,5} The involvement of surface As atoms in bonding to oxygen has been firmly established by the observation of a well-resolved chemical shift in the As $3d$ level following oxygen adsorption.^{2,3,5} The involvement of surface Ga atoms, however, is unclear because only a broadening in the Ga $3d$ level is observed following oxygen adsorption. The interpretation of the broadening in the Ga $3d$ is not straightforward. Brundle and Seybold³ have proposed the direct growth of Ga_2O_3 , as the magnitude of chemical

shifts are close to those expected for the two bulk oxides. Pianetta *et al.*⁵ have suggested that (As,O) bonding could induce broadening in the Ga $3d$ level. For oxygen bonding only to the surface As, Barton and Goddard⁴ have calculated an (As,O) bonding-induced shift of 0.8 eV in the Ga $3d$ level in addition to a 2.6-eV shift in the As $3d$ level; these shifts agree well with experiments.^{2,3,5} Such divergence of interpretations illustrates the difficulty in attaining an unambiguous answer from the magnitude of the shifts in core level alone.

In this work, we turn our attention to the density of valence states (DOVS) of the GaAs(110) surface adsorbed with oxygen (that produced by exposure to unexcited oxygen⁵ at room temperature, hereinafter referred to as the DOVS of O-GaAs). We will also compare DOVS's obtained from oxygen adsorption on a variety of surfaces. It will be seen that careful examination of the DOVS can often resolve the ambiguities associated with the core-level spectra. After describing the experimental details in Sec. II, the results of oxygen adsorption on cleaved GaAs(110) will be given in Sec. III.

Particular emphases are given to the 30-eV spectra which are better representations of the DOVS than spectra obtained with lower photon energies. Coverage-dependent features and the substrate features in the 30-eV spectra are carefully separated out in order to obtain a representation of the DOVS of O-GaAs(110). An interpretation of the DOVS obtained this way will be offered based on comparisons made with the experimental DOVS' of Ga₂O₃ and As₂O₃. In Sec. IV we will present results of oxygen adsorption on sputter-disordered GaAs surfaces. The understanding of the adsorption process on the disordered surfaces provides great insights into the adsorption process on ordered surfaces. The photoemission spectra obtained for oxygen adsorption on disordered surfaces also serve as useful references for interpreting photoemission spectra obtained under other conditions. In Sec. V, studies are made on surfaces which were first covered with oxygen and then annealed to elevated temperatures. Such annealing studies reveal the stability of the bondings formed by room-temperature adsorption.

II. EXPERIMENTAL

Experiments were performed in a stainless-steel ultrahigh vacuum chamber with base pressure $\sim 10^{10}$ Torr. The light sources used include synchrotron radiations from the 8° and the 4° beam lines of the Stanford Synchrotron Radiation Laboratory (SSRL),¹⁰ and monochromatized He I (21.2-eV), He II (40.8-eV) radiations from a He discharge. The O 1s spectra were obtained with Mg K α emission ($h\nu = 1253.6$ eV). Energy analyses of photoelectrons were performed with a double-pass cylindrical mirror analyzer (Physical Electronics). Combined monochromator-analyzer energy resolutions are 0.2 eV for 21-eV spectra, 0.3 eV for 30-eV spectra, 0.35 eV for 100-eV spectra, 0.3 for He I spectra, and 0.4 eV for He II spectra.

Research grade oxygen was used in making the oxygen exposures. Unless otherwise stated, oxygen exposures were made with all the precautions necessary to avoid generating excited oxygen which could lead to different oxygen adsorption process.⁵

The heatings were achieved by a tungsten filament which was enclosed in the molybdenum sample holder positioned at the back end of the crystal. To avoid contamination during heating the heaters had been thoroughly outgassed to temperature $\geq 550^\circ\text{C}$ prior to the heating experiments. Temperatures were monitored with a thermocouple

mounted near the back end of the crystals and an infrared pyrometer focused near the crystal surfaces. A consistent temperature scale for different experiment runs was obtained from the pyrometer readings. The discrepancies in the thermocouple reading from different experiment runs, however, place the accuracy of the quoted temperature to $\pm 300^\circ\text{C}$. (The reproducibility of a given temperature, however, is much better.)

Samples used in this work are assigned identification such as *N* 1, *N* 2, *P* 1, etc., with the characters *N* and *P* indicating *n*-type and *p*-type samples, respectively. The crystal suppliers and the doping concentrations are as follows: samples *P* 1–*P* 4, 1.8×10^{18} cm⁻³ Zn doped, laser diode; samples *N* 1–*N* 5, 4×10^{17} cm⁻³ Sn doped, Varian Associates; samples *N* 6–*N* 8, 5×10^{17} cm⁻³ Te doped, Crystal Specialty; samples *N* 9–*N* 12, 5×10^{18} cm⁻³ Si doped, laser diode.

III. RESULTS AND DISCUSSION OF ROOM-TEMPERATURE ADSORPTION ON CLEAVED GaAs(110)

In this section we present results of room-temperature adsorption on cleaved GaAs(110) surfaces. Emphasis is given to the valence-band spectra, but a summary of the results from the core-level spectra will be given in Sec. III A. Experimental valence-band spectra of O-GaAs(110) are presented in Sec. III B. The different coverage dependence of the various features in the spectra are carefully analyzed in Sec. III B. Contributions to the valence-band spectra from two different forms of adsorbed oxygen are separated from each other by such analyses. The interpretation of the spectrum of the major chemisorption form—oxygen which adsorb on normal surface sites and produce chemical shifts in the core level—is attempted in Sec. III C. The nature of another form of oxygen is discussed in Sec. III D. Some speculations about the mechanism of adsorption, particularly the role of defects in the initial steps of adsorption, are given in Sec. III E.

A. Results from core-level spectra

The basic facts available in the core-level spectra have been reported by Pianetta *et al.*⁵ We have repeated the measurements of Pianetta *et al.* with improved energy resolution and signal-to-noise ratio. An overview of the Ga 3*d* and the As 3*d* levels

of GaAs(110) surfaces subjected to a sequence of oxygen exposures is given in Fig. 1. All important features reported by Pianetta *et al.* are reproduced: (1) no chemical shift in either the As 3d or the Ga 3d can be clearly observed for oxygen exposures smaller than about 10^7 L (1 L = 10^{-6} Torr \times 1 sec), (2) a well-resolved chemical shift ($\Delta E = 3.0 \pm 0.1$ eV—quoted as 2.9 eV in Ref. 5 and other work) in the As 3d is observed for oxygen exposures higher than about 10^7 L, and (3) the full width at half-maximum (FWHM) of the Ga 3d level increases with increasing exposure, but no clearly resolvable shift can be observed throughout the whole exposure range we have studied.

The broadening of the Ga 3d level is further examined in Fig. 2, where the Ga 3d and the As 3d spectra of the clean surface are subtracted from those of the oxidized surface (10^{10} -L exposure). The subtraction was done by aligning the unshifted As 3d in the two spectra in energy and by adjusting intensities of the two spectra to have equal areas under the unshifted As 3d. The difference curve (the bottom curve, Fig. 2) shows two peaks in the Ga 3d region, whereas the intensity in the energy region of the unshifted As 3d is, of course, zero. One of the two peaks in the Ga 3d region has binding energy (BE) higher than that of the unshifted Ga 3d while the other has lower BE. Be-

cause oxygen adsorption induced both a high BE component and a low BE component in the Ga 3d, Pianetta *et al.*⁵ have described it as “homogeneous” broadening. The difference curve in Fig. 2, however, clearly indicates that the broadening is asymmetrically toward the high BE side.

There are two possible explanations for the appearance of a component shifted to the low BE side as well as a component shifted to the high BE side. The first is that the assumption that $E_b(\text{As } 3d) - E_b(\text{Ga } 3d)$ of the component unshifted levels remains constant with oxygen adsorption is invalid. In the spectrum of a clean GaAs(110) surface, there are contributions from both atoms in the surface layer and atoms in the bulk. Eastman *et al.*¹¹ have found that the BE's of the As 3d and the Ga 3d of the surface atoms are different from those of the atoms in the bulk. Thus, the value of $E_b(\text{As } 3d) - E_b(\text{Ga } 3d)$ observed on a clean relaxed GaAs(110) surface is different from that expected in the absence of surface shifts. Assuming the surface atoms contribute 50% intensity to the observed spectrum and using the values of surface shifts of Eastman *et al.*,¹¹ the observed $E_b(\text{As } 3d) - E_b(\text{Ga } 3d)$ is estimated to be 0.33-eV smaller than in the absence of surface shifts. Assuming the oxygen adsorption removes the surface shifts, the value of $E_b(\text{As } 3d) - E_b(\text{Ga } 3d)$ would be changed following

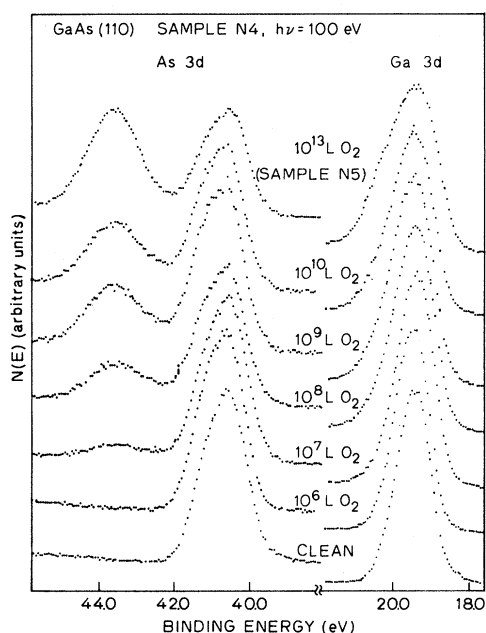


FIG. 1. As 3d and Ga 3d levels of clean and oxygen-exposed *n*-GaAs(110) measured at $h\nu = 100$ eV. The 10^{13} -L spectrum was obtained on a different surface.

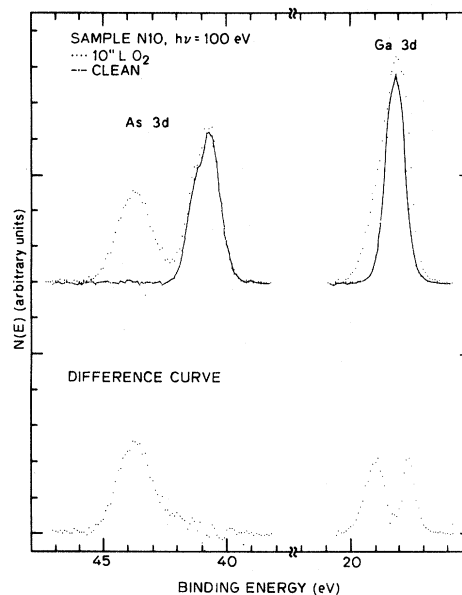


FIG. 2. Difference curve between the As 3d and the Ga 3d spectra of clean and oxygen-exposed *n*-GaAs(110). Notice that oxygen exposure induced broadening in the Ga 3d toward both the low-energy side and the high-energy side.

oxygen adsorption. We have indeed found it possible to eliminate the low BE component of the shifted Ga 3*d* in the difference curve by increasing the value of $E_b(\text{As } 3d) - E_b(\text{Ga } 3d)$ by 0.4 eV after oxygen adsorption. We should also notice that for this explanation to hold the removal of the surface shifts has to occur at an oxygen coverage significantly below monolayer. This is because the low BE component of the shifted Ga 3*d* appears following exposure as low as 10^8 L ($\Theta \approx 0.4$ monolayer). In low-energy electron diffraction LEED *I-V* studies,⁶ the *I-V* structure characteristic of an ideally relaxed GaAs(110) surface was found to be drastically modified after an exposure of 10^8 L. It is thus conceivable that the surface shifts, which are directly related to the long-range relaxation of the GaAs(110) surface,¹¹ are lost after an exposure of 10^8 L or less.

Another possible explanation is simply that the adsorption of oxygen induces a broad shifted Ga 3*d* peak which extends to both the high BE and the low BE side of the unshifted Ga 3*d*. This explanation is reasonable especially in view of findings from the oxidation of pure Ga.¹² There the Ga 3*d* of clean Ga metal is found to show well-resolved spin-orbit splitting. Such resolvable splitting is absent for either the Ga 3*d* of clean GaAs or the Ga 3*d* of GaAs adsorbed with oxygen or the Ga 3*d* of Ga₂O₃. The FWHM of the Ga 3*d* of Ga₂O₃ is also significantly larger than that of clean Ga.¹²

At the present, we do not have experimental data to distinguish the two possibilities. The complex oxygen-induced change in the Ga 3*d* as revealed in Fig. 2, however, illustrates the difficulty in interpreting the core-level spectra of adsorption at surfaces.

The amount of shifted As 3*d* and shifted Ga 3*d* at various oxygen exposures, expressed, respectively, as a percentage of the total As 3*d* emission and the total Ga 3*d* emission, are listed in Table I. The amount of shifted Ga 3*d* were estimated using

three methods: (1) measure the area under the shifted Ga 3*d* in the difference curve, (2) fit the Ga 3*d* peak with three skewed Gaussians, one unshifted (which remains the same BE relative to the As 3*d* as on the clean surface) and two shifted (toward higher BE and lower BE), and (3) fit the Ga 3*d* with two components, one "unshifted" and one shifted toward higher BE (the position of the "unshifted" component was also permitted to vary in the fitting procedure). All three methods agree within 10%. We notice that for all exposures, the percentage of shifted As 3*d* is roughly the same as the Ga 3*d*.

It is also interesting to notice that the percentage of shifted As 3*d* at 10^{13} -L exposure is about the same as that reported by Pianetta *et al.*⁵ at 10^{12} -L exposure. Since only two data points are available, it is not clear if a saturation of the adsorption process is reached between 10^{12} and 10^{13} L, although the data are suggestive of this. (In on-going work in our laboratory, much higher oxygen coverage than the highest observed here was found obtainable by irradiating the GaAs surface with Ar laser during oxygen exposure,¹³ "saturation" at one monolayer therefore may not be an important characteristic of the room-temperature chemisorption phase to be discussed here; this is contrary to the suggestion made in Refs. 2 and 5.) The escape-depth analyses of Pianetta *et al.*, however, have indicated that it is reasonable to assume the 52% shifted As 3*d* corresponds to the adsorption of one monolayer of oxygen. This assumption is adopted here and is used in estimating the oxygen coverages at various exposures; these estimates are listed in Table I. The intensity of the O 2*p* normalized to the intensity of the Ga 3*d* at each exposure is also entered in Table I for later comparisons.

The fact that the shift in the As 3*d* is constant at any coverage below one monolayer (Fig. 1) is worth emphasizing: It indicates that the oxygen

TABLE I. Percent of shifted As 3*d* and Ga 3*d* at various exposures.

Treatment	Percent shifted As 3 <i>d</i>	Percent shifted Ga 3 <i>d</i>	Intensity O 3 <i>d</i>	Coverage (monolayer)
10^7 L O ₂	9	12	0.09	0.17
10^8 L O ₂	23	22	0.16	0.35
10^9 L O ₂	27	26	0.26	0.5
10^{10} L O ₂	34	28	0.33	0.65
10^{13} L O ₂	52	47	0.49	1.0

coordination number of As in the O-GaAs(110) bonding is constant with increasing oxygen coverage.

B. Valence-band spectra

Overviews of the valence-band spectra of an *n*-GaAs(110) surface subjected to a sequence of oxygen exposures, taken at 21- and 30-eV photon energies, are displayed in Figs. 3 and 4, respectively.

The major oxygen-induced feature seen in the 21-eV spectra is a relatively sharp peak at 4.6 ± 0.1 eV below the valence-band maximum (VBM). Because of the relatively long escape depth of the photoelectrons excited by this photon energy from it, the peak (6.9-eV BE) due to the *s-p* hybrid band of bulk GaAs is also seen in all spectra. Knowledge of the energy position of this peak relative to the Fermi level is useful in determining the band bending in GaAs induced by oxygen adsorption (to be discussed in the Appendix). The energy separation between the oxygen peak (4.6-eV BE) and the substrate peak (6.9-eV BE) is constant with increasing oxygen exposures. This reflects the same fact that is given by the constant energy separation between shifted and unshifted As 3*d* peaks, namely, the oxygen substrate bonding is probably coverage independent. In addition, this separation is the same for an *n*-type sample and a *p*-type sample whose surface Fermi-level positions in the band

gap are significantly apart (~ 0.4 eV) from each other at low energy coverages (< 0.6 monolayer). This is seen in Fig. 5 where we have displayed the 21-eV spectra obtained on a *p*-type sample, with the Fermi-level position indicated in each spectrum. Therefore, the binding energy of the oxygen peak is a constant when referenced to the valence-band maximum of the GaAs substrate, but not a constant when referenced to the surface Fermi level. If room-temperature adsorption of oxygen on GaAs(110) resulted in the direct formation of islands of bulk oxides ($\text{As}_2\text{O}_3, \text{Ga}_2\text{O}_3$) that are chemically separated from the substrate, the change in band bending within the GaAs substrate is not expected to affect the binding energy of oxygen levels referenced to the Fermi level. Thus, an oxygen-substrate bonding configuration with oxygen atom "continuing" or "inserted into" the lattice conforms better to the above observation than the formation of oxide islands.

In the 21-eV spectra some oxygen-induced features at higher binding energy may be shadowed by the secondary electron emission. The secondary background in the region of interest is greatly reduced in the 30-eV spectra. As an example, the As 4*s*-like band of clean GaAs(110), which cannot

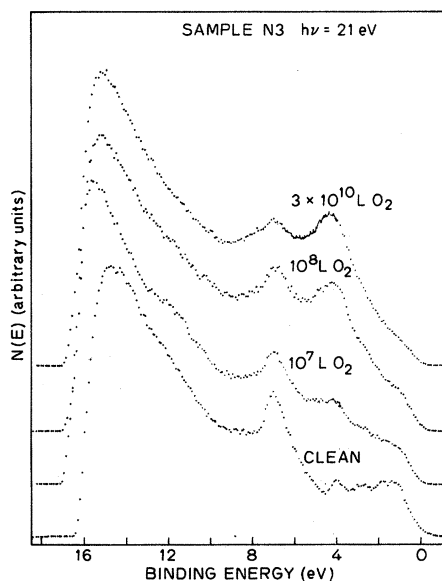


FIG. 3. Photoemission spectra of clean and oxygen-exposed *n*-GaAs(110) obtained at $h\nu = 21$ eV.

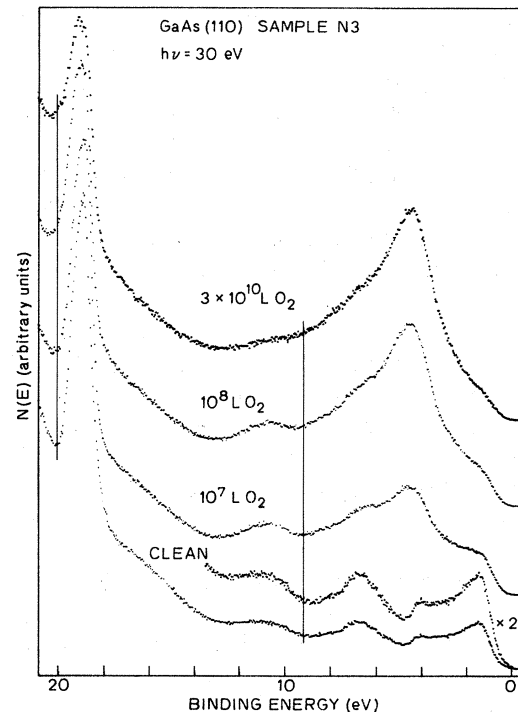


FIG. 4. Photoemission spectra of clean and oxygen-exposed GaAs(110) obtained at $h\nu = 30$ eV.

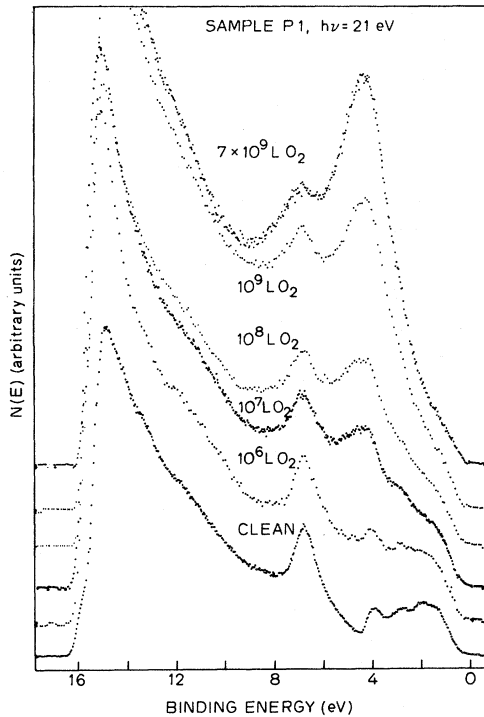


FIG. 5. Photoemission spectra of clean and oxygen-exposed *p*-GaAs(110) obtained at $h\nu=21$ eV. The 10^9 -L exposures were made with excited oxygen.

be unambiguously identified in the 21-eV spectrum, is clearly discernable in the 30-eV spectrum (~ 11 -eV BE). The 30-eV spectra also give increased cross section for oxygen levels and decreased cross section for substrate features, when compared to the 21-eV spectra, the *s-p* mixed band (6.9-eV BE) in the 10^7 -L $\sim 3 \times 10^{10}$ L spectra in Fig. 4. The density of valence states of O-GaAs(110) is therefore better represented by the 30-eV spectra.

To further reveal details in the DOVS of O-GaAs(110), we have obtained a few difference curves which are shown in Fig. 6. Panel (a) gives the difference curve between the 10^7 -L spectrum and the clean spectrum of sample *N3* (the bottom curve). The original spectra with smooth and featureless backgrounds removed are also shown in the top part of panel (a). The subtraction necessary for obtaining the difference curve is done in such a way that (i) zero intensity is reached in the difference curve at the energy position corresponding to the clean component of the Ga *3d* level (not shown in Fig. 6), and (ii) the intensity of the leading peak of the clean spectrum and the intensity of the shoulder near VBM in the 10^7 -L spectrum are adjusted to be about equal before the subtraction.

The difference curve between the 3×10^{10} -L spectrum and the clean spectrum is obtained in a similar way and is shown in panel (b). The two difference curves in panels (a) and (b) are compared in panel (c). Overall resemblance can be seen between the two difference curves in the BE region 0–10 eV. The relative heights of the major oxygen peak and the feature in the 10–12-eV BE region [labeled *S* in panel (c)], however, are quite different in the two difference curves. An examination of Fig. 4 shows that feature *S* does not grow with increasing oxygen exposure as the 4.6-eV peak does. This is verified by the difference curve taken between the 3×10^{10} -L spectrum and the 10^7 -L spectrum, which is shown in panel (d). In that difference curve, little intensity is seen in the region between 10- and 12-eV BE, where feature *S* appears in the 10^7 -L clean difference curve. Feature *S* is attributed to a different form of oxygen which saturates at low exposure and low coverage. More detailed discussion of this low-coverage state will be postponed until Sec. III D. Sufficient to point out here that the difference curve given in panel (d) is a true representation of the DOVS of the major form of adsorbed oxygen, i.e., the adsorbed oxygen that produce the chemical shifts in As *3d* and Ga *3d* discussed in Sec. III A. The DOVS in panel (d) consists of a prominent peak at 4.6-eV BE and a broad shoulder in the region of 6.5–10-eV BE. Interpretations of these features will be given in Sec. III C.

C. Interpretation of the DOVS

The first piece of information to be drawn from the DOVS shown in Fig. 6(d) is that oxygen adsorb dissociatively on the GaAs(110) surface. Molecular species such as O_2^- , O_2^{2-} , are expected to give multiplets with comparable strength in the photoemission spectrum.¹⁴ Mele and Joannopoulos¹ in their tight-binding calculations have found three molecular levels of comparable strength, with binding energies of 4, 8, and 10 eV for peroxy radicals chemisorbed on either Ga or As sites, and with binding energies of 4, 8, and 12 eV for peroxide bridge bridging over second-nearest Ga and As atoms. The DOVS in Fig. 6(d), showing a single dominant peak at 4.6-eV BE, gives no reminiscence of the multiplets characteristic of the O–O bonding. We therefore conclude that nondissociative chemisorption, either in the form of peroxy radical or in the form of peroxide bridge, does not occur

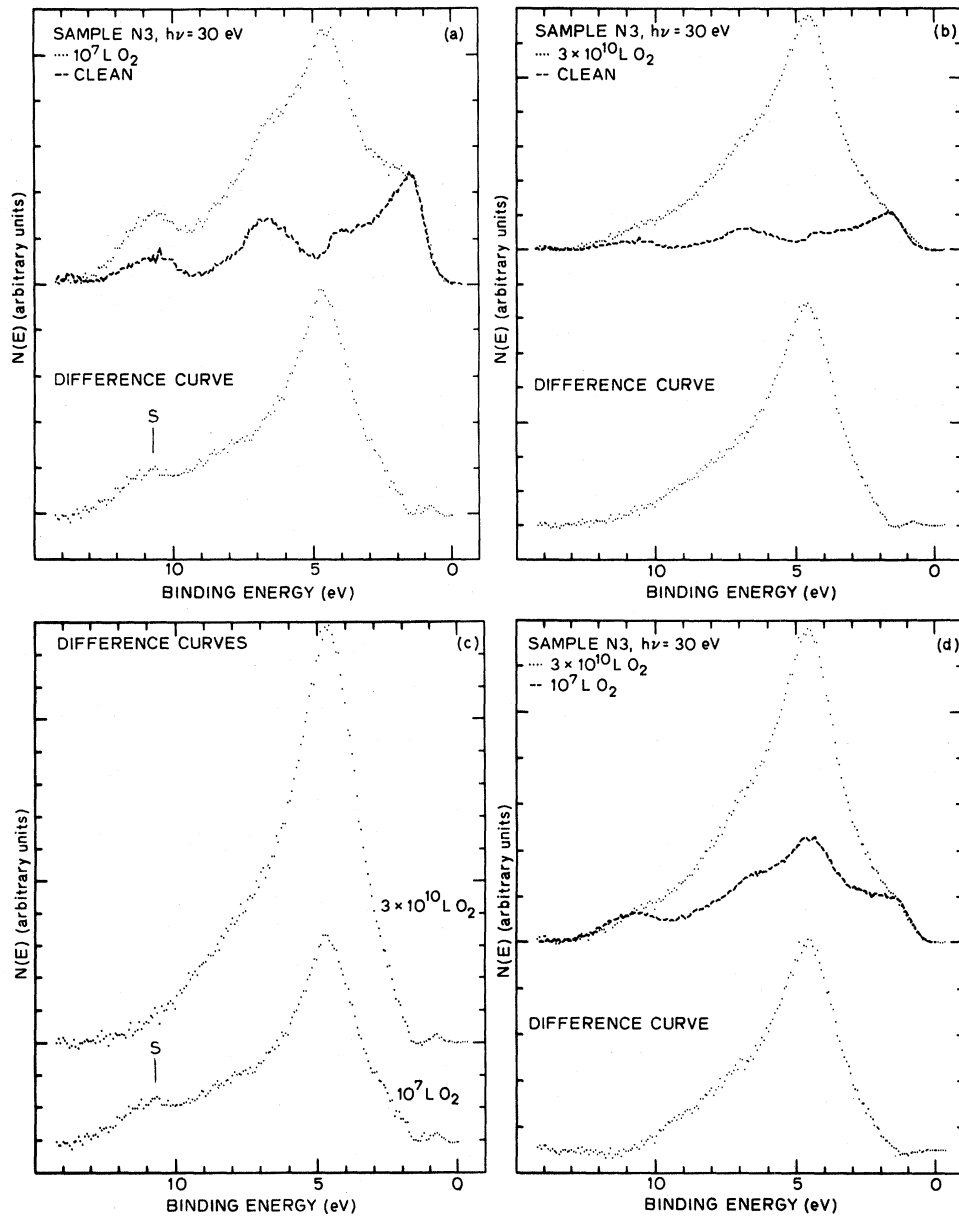


FIG. 6. Difference curves between the spectra of clean and oxygen-exposed surfaces at two different exposures are obtained in (a) and (b). When these two difference curves are compared in (c), coverage-dependent variations in the spectra are revealed. The coverage-dependent features can be removed by taking difference between the high-coverage and the low-coverage spectra (d).

for room-temperature adsorption of oxygen on GaAs(110) surfaces. The same conclusion has been reached by Brundle and Seybold³ based on the binding energy of the O 1s level.

Having established that the adsorption is dissociative, the DOVS can be described in general terms of the bonding properties of the oxygen atom. There are four electrons in the *p* shell of an oxygen atom leading to one doubly occupied and two singly occupied *p* orbitals. Only the two singly occu-

ried *p* orbitals participate in the bonding of the oxygen atom to other atoms, and the doubly occupied *p* orbital remains nonbonding. The essential feature of the DOVS of any oxide therefore consists of a nonbonding band and a bonding band. A simple characterization of such DOVS can be made in terms of two parameters: the energy splitting between the nonbonding and the bonding bands (hereinafter referred as *N-B* splitting), and the ratio of the density of the nonbonding and

bonding states (hereinafter referred to as the $N-B$ ratio). For example, when the oxygen atom is in a bridge bonding position, the $N-B$ ratio 1:2 based on simple counting of the nonbonding and the bonding electrons. In practice, however, both the $N-B$ splitting and the $N-B$ ratio may be difficult to extract from the experimental DOVS. For example, the different matrix elements for the photoionization of the nonbonding and the bonding orbitals may make the density ratio ambiguous; the broadening in the bonding band due to the disorder of the oxides may cause difficulty in determining the energy splitting between the nonbonding and the bonding bands.

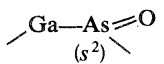
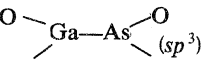
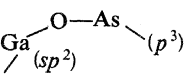
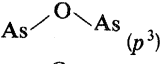
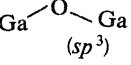
To avoid the difficulties in extracting absolute numbers for the $N-B$ splitting and the $N-B$ ratio from the experimental DOVS's, the approach to be used below is to qualitatively compare the $N-B$ splitting and the $N-B$ ratio between the DOVS's of several possible oxygen bonding configurations. In particular, we will compare the DOVS of O-GaAs(110) to the DOVS's of As_2O_3 and Ga_2O_3 .

As a first step of comparing the experimental DOVS's, we have theoretically projected (using methods to be immediately described) the two parameters (the $N-B$ splitting and the $N-B$ ratio) of a few possible oxygen bonding configurations and have listed the results in Table II. Configurations As-O-As (IV) and Ga-O-Ga (V) are included to simulate the known oxides As_2O_3 and Ga_2O_3 , respectively, in calculating the $N-B$ splittings. Configurations I-III are candidates to be considered for the O-GaAs(110) bonding. In configuration I of Table II, the oxygen atom terminates a

doubly occupied surface As dangling orbital; the As=O bonding involves π as well as σ interactions, as discussed by Lucovsky and Bauer¹⁵ and Barton *et al.*⁴ In configuration II the oxygen terminates a singly occupied sp^3 hybrid of As or Ga or both; this configuration has been examined in detail by Mele and Joannopoulos¹ with tight-binding calculations. In configuration III the oxygen atom breaks a surface bond and bridges over a pair of nearest-neighbor Ga and As.

The $N-B$ ratios given in Table II are based on simple counting of bonding and nonbonding electrons. No distinction is made between s electrons (contributed by the Ga or the As to the bonding band) and p electrons, although in our condition ($h\nu=30$ eV) p electrons may be preferentially emphasized over s electrons in the measured DOVS's. Such error, however, is expected to be the same for all bonding configurations considered in Table II. As mentioned above, in configuration I the two doubly occupied O $2p$ orbitals have π interaction with the empty $4d$ orbitals of As.^{4,13} The π interaction, however, is weaker than the σ bonding, hence we expect a splitting between the π and σ bondings. We will therefore count electrons in the donorlike π bonding as "nonbonding." The nonbonding to bonding electrons ratio for configuration I is the highest in Table II. For oxygen in bridge position, the $N-B$ ratio is 1:2 in all cases (configurations III through V). In bulk Ga_2O_3 , complication arises because some oxygen lone pairs can interact with nearby empty Ga orbitals and form donorlike bonds (see Ref. 12 for more details). This complication has been ignored in Table

TABLE II. Qualitative trends in the characteristics of the DOVS's of a few oxygen-bonding configurations.

No.	Bonding configuration	$N-B$ splitting (eV)	$N-B$ ratio
I		3.36	2:1
II		O-Ga 5.75 (2.5 ^a) O-As 7.04 (6.0 ^b)	3:2
III		5.19	$\begin{cases} \pi:2.86 \\ \sigma:7.52 \end{cases}$ 1:2
IV		4.85	$\begin{cases} \pi:2.76 \\ \sigma:6.94 \end{cases}$ 1:2
V		5.62	$\begin{cases} \pi:4.10 \\ \sigma:7.15 \end{cases}$ 1:2
	As_2O_3	(expt.)3.3	$\begin{cases} \pi:2.41 \\ \sigma:4.18 \end{cases}$
	Ga_2O_3	(expt.)~4.5	

^aCalculated values of Mele and Joannopoulos (Ref. 1).

II, but it is discussed below when making comparisons of the experimental DOVS.

Simple linear combination of atomic orbitals (LCAO) calculations, similar to that done for Si—O—Si by Harrison,¹⁶ have been performed to obtain the N - B splittings in Table II. These calculations were done only to reveal the trend in the N - B splitting among the various configurations considered. No absolute correspondence between these numbers and the experimental DOVS should be sought. Some of the details of the calculation can be found in the Appendix. We notice here that for configurations containing bridge oxygen (III—V) the bonding band further splits into a σ component and a π component. Broader bonding bands are therefore expected for configurations III—V when compared to configuration I. In Table II, we have listed the centers of gravity of σ and π components as the N - B splittings for configurations III—V; splittings between the nonbonding oxygen orbital and the individual σ and π components are enclosed in parentheses. The following trends in the theoretical N - B splittings are observed:

(i) Configuration I has the smallest N - B splitting and the narrowest bonding band among all the bonding configurations considered in Table II.

(ii) Single As (sp^3) hybrid to oxygen gives an N - B splitting even bigger than those expected for As_2O_3 and Ga_2O_3 .

(iii) The N - B splitting for the Ga—O—As bridge is intermediate between that of As—O—As and that of Ga—O—Ga, or it is intermediate between the N - B splittings of As_2O_3 and Ga_2O_3 .

In Fig. 7, we compare the experimental DOVS of As_2O_3 (top) and Ga_2O_3 (bottom) to that of oxygen adsorbed on GaAs(110) [center, reproduced from Fig. 6(d)]. All the three spectra are displayed with the Fermi level as the energy zero. The DOVS's of As_2O_3 and Ga_2O_3 were obtained using the same spectrometer used in this work; more detailed discussion of these DOVS's will be given in Refs. 12 and 17. Here we can make the following qualitative observations.

(i) The bonding band of the DOVS of oxygen adsorbed on GaAs(110) is not as pronounced as those of the DOVS's of As_2O_3 and Ga_2O_3 . The comparison made with the DOVS of Ga_2O_3 is somewhat ambiguous due to the presence of the donorlike bonding band.¹² The comparison made with the DOVS of As_2O_3 , however, is clear. This suggests the importance of nonbridging oxygen (configurations I or II) bonding for oxygen chem-

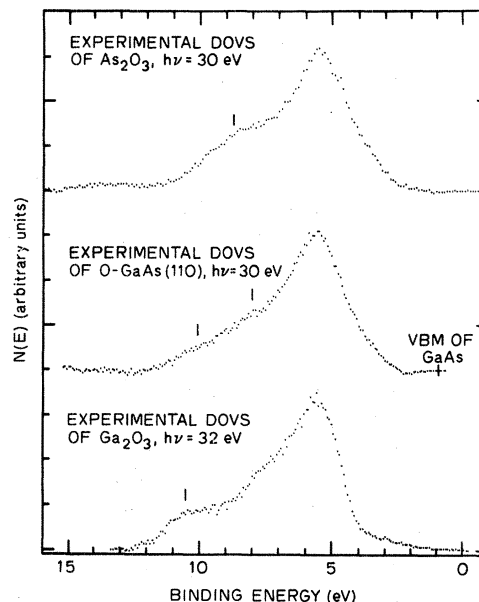


FIG. 7. Comparison of the experimental DOVS of O-GaAs(110) (center) to those of As_2O_3 (top) and Ga_2O_3 (bottom). The DOVS's of O-GaAs(110) and As_2O_3 were obtained at $h\nu=30$ eV, whereas that of Ga_2O_3 was obtained at $h\nu=32$ eV.

isorbed on GaAs(110).

(ii) There is no component of the bonding band of the DOVS of O-GaAs(110) that has an N - B splitting bigger than that of Ga_2O_3 . This, according to Table II, disfavors configuration II. The same conclusion is reached by comparing the more accurate tight-binding values¹ to experimental DOVS. We therefore suggest that, in conjunction with (i), As=O (instead of Ga—O, As=O) is the important nonbridging oxygen binding to consider.

(iii) The bonding band in the DOVS of O-GaAs(110) is broad and its high-binding energy edge lies at a binding energy higher than that in the DOVS of As_2O_3 but comparable to that in the DOVS of Ga_2O_3 . This suggests other types of bonding As=O. In Sec. IV below we will give evidence showing that Ga—O—Ga, and hence As—O—As, bonds are unlikely to result from room-temperature adsorption of oxygen on GaAs(110). The Ga—O—As bridge is therefore important to consider in addition to the As=O bonding. The specific way the As=O and the Ga—O—As bondings is mixed cannot be deduced from the DOVS of O-GaAs(110). Suggestions, however, can be made below by bringing together all available data.

In Fig. 8, we suggest an adsorption configura-

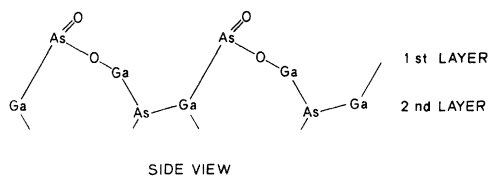


FIG. 8. Proposed bonding model for room-temperature adsorption of oxygen on GaAs(110). A side view of the (110) surface is shown here.

tion consisting of an oxygen atom datively bonded (i.e., the As=O bond¹⁵) to a surface As and an oxygen atom inserted into one of the back bonds to the same surface As. Further explanations of the motivations for this suggestion will be pointed out in Sec. III E where we discuss the adsorption mechanism. Here, we only notice that the model is not inconsistent with the chemical shifts in core levels: a surface As atom is bonded to two oxygen atoms but with three electrons participated in bonding, hence the chemical shift is comparable to that found¹² for As₂O₃; a surface Ga atom is bonded to only one oxygen atom, hence a small and unresolved chemical shift in the Ga 3*d* level.

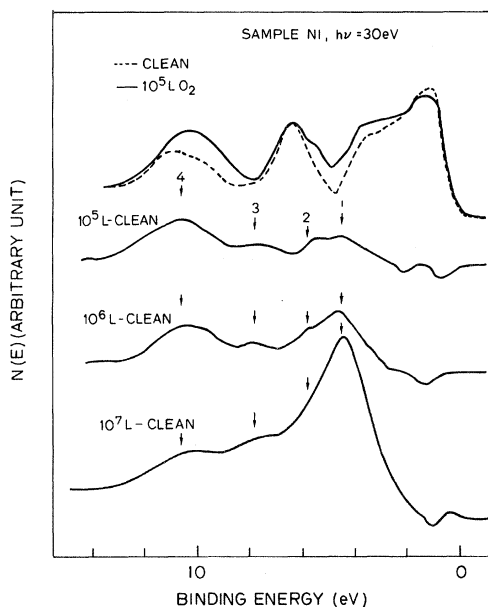


FIG. 9. Photoemission spectra of a clean *n*:GaAs(110) (top curve) and the difference curves between spectra of clean and oxygen-exposed surfaces at a sequence of oxygen exposures. The spectra were obtained at $h\nu=30$ eV. Features 1 and 3 are associated with one form of oxygen, and 2 and 4 with another.

D. The low-coverage adsorption state

We now return to discuss the feature between 10–12-eV BE in Fig. 6. In Fig. 9 we show the spectrum of a clean GaAs(110) (top curve, dashed) and the difference spectra (the oxygen-exposed minus the clean) of this surface subjected to three different oxygen exposures. The same feature between 10–12-eV BE (labeled 4 in Fig. 9) is seen in the 10⁵-L difference spectrum. This feature probably is shadowed by the 4.6-eV BE nonbonding oxygen peak in high-exposure spectra shown in Fig. 6. Feature 1 is weak and feature 3 appears nearly in the noise level in the 10⁵-L difference spectrum, but they are clearly the dominant features in the 10⁷-L spectrum. (The basis for associating feature 3, a broad shoulder, with peak 1 is better seen in the sequence of difference curves in Fig. 6 than in Fig. 9.) Features 1 and 3 are the key features of the major chemisorbed species, as discussed in Sec. III C. Features 2 and 4 are therefore associated with a different oxygen state which, according Fig. 9, saturates at $\leq 10^5$ -L exposure. The saturation coverage of this state can be estimated in the following way: the intensity of emission from features 2 and 4 in the 10⁷-L spectrum is less than 10% of that due to features 1 and 3 (features of the chemisorption state). The oxygen coverage of the major chemisorption state is approximately 0.1 monolayer for a surface exposed to 10⁷-L oxygen (Table I, Sec. III A). Thus, the saturation coverage of the low-exposure state is less than 0.01 monolayer.

The low-saturation coverage reached with low exposure suggests that the adsorption of this state of oxygen may be at surface-defect sites. Some clues to the nature of this state and the nature of the defect sites are given below.

The binding energies of features 2 and 4, 5.3 and ~ 10.3 eV, respectively, are the same as those found for Ga–O–Ga bridge bonds (to be discussed in the next section, where a large number of such bonds are found on a sputter-disordered Ga-rich GaAs surface). Heating experiments (to be discussed in Sec. IV) also revealed that this low-coverage state of oxygen desorbs at $\sim 150^\circ\text{C}$, which is consistent with the high volatility of Ga₂O. This low-coverage state of oxygen is therefore interpreted as oxygen bridge-bonded over two closely positioned Ga atoms. This interpretation is consistent with the results of Thuault *et al.*¹⁶ They have found, using photoemission yield spectroscopy, that a partially filled band of Ga-derived defect states present on cleaved GaAs(110) can be

removed by oxygen exposure as low as 1 L.

The types of surface defects that can give the partially filled Ga-derived states observed by Thuault *et al.*¹⁸ and that can easily form the Ga—O—Ga bonding are, for example, surface As vacancies or Ga terminated steps or As vacancies at steps. (This suggestion is supported by the following interatomic distance: the shortest Ga—Ga distance in Ga—As is 3.99 Å, and the Ga—Ga distance in the Ga—O—Ga unit of Ga₂O₃ is 3.45 Å.) The detailed nature of the defects on cleaved GaAs(110) surfaces remains to be determined by other methods. However, it is important to point out that we have obtained (via oxygen adsorption) a signature of an important class of defects on cleaved GaAs(110).

E. Discussion of the possible adsorption mechanisms

Suggestions have been made in the past that the dissociation of molecular oxygen on GaAs(110) occurs at defect sites.³ The identification of the low-coverage state of oxygen indicates that one important (possibly the most important) class of defects on GaAs(110) are passivated by oxygen before the major chemisorption state emerges. This observation suggests that the role of defects in the dissociative adsorption of oxygen (the high-coverage state) on GaAs(110) may be insignificant. Dissociation of molecular oxygen at defect sites has been proposed to control the kinetics of gas adsorption on many metal surfaces.¹⁹ In that picture, oxygen molecules are dissociated at defect sites and the dissociated oxygen atoms migrate away to bond at normal surface sites (i.e., surface sites defined by the ideal surface lattice, including reconstruction or relaxation if that occurs). On semiconductor surfaces, a picture with much more localized reactions may apply. That is, oxygen molecules dissociated at defect sites also react with atoms surrounding the defect sites, thus leading to the passivation of the defect sites in the rest of the adsorption process. This picture of localized reaction clearly applies to the low-coverage-adsorption state (Sec. III D) which we have observed on GaAs(110). Although other types of defects capable of nonlocalized dissociation reaction may exist on GaAs(110) without being detected, the present finding at least suggests that localized reaction of oxygen at defect sites is important to consider.

Defect sites on semiconductor surfaces may enter the oxygen adsorption process in another

way. Mark *et al.*²⁰ have proposed that defect sites on GaAs surfaces serves as the nucleation centers for the oxidation process. In that picture, oxygen molecules dissociate and react locally at defect sites, but the heat of adsorption induces more defect sites around these defect sites and the oxidation process continues on. In Sec. IV below we will show that on sputter-disordered GaAs(110) surfaces, where gross disorder is introduced such that there are more defect sites than normal sites, the adsorption of oxygen is separated in two distinct steps: oxygen first adsorbs on defect (Ga-rich) regions to saturation, and then adsorbs on normal sites with a rate comparable to that found on ordered GaAs(110). As explained in Sec. III D, the same two-site oxygen adsorption occurs on cleaved, ordered GaAs(110), only that the amount of oxygen adsorbed on defect (As-deficient) sites is much smaller. Since the numbers of oxygen atoms adsorbed in the first step (i.e., onto As-deficient sites) on ordered and disordered surfaces are proportional to the numbers of defect (As-deficient) sites that are present on the two surfaces before oxygen adsorption, it is reasonable to assume that adsorption on the two layers of sites are independent of each other. This suggests that the picture of Mark *et al.*²⁰ may be inappropriate for the adsorption of oxygen on GaAs(110).

The above discussion was meant to point out that the dissociation of oxygen molecules does not necessarily occur through interactions with defect sites. In Fig. 10(a) a possible mechanism of dissociating oxygen molecules at normal surface sites of GaAs(110) is suggested. On perfect, relaxed GaAs(110) the most easily accessible electrons for impinging oxygen molecules are those in the As lone pairs, hence an impinging oxygen molecule is forced to interact with an As lone pair. That interaction is then assumed to lead to the formation

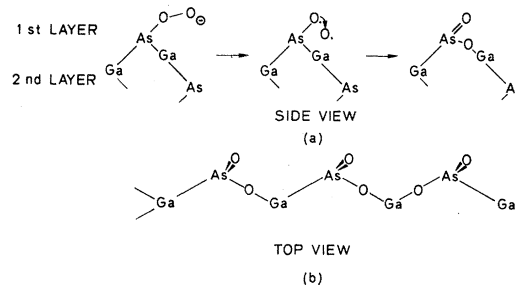


FIG. 10. (a) Proposed mechanism of the dissociation of oxygen molecules on GaAs(110) surfaces. (b) Top view of the proposed bonding model, showing that the oxygen coordination number of surface Ga may vary between 1 and 2.

of a peroxy zwitterion, as shown on the left of Fig. 10(a). The peroxy zwitterion is highly unstable because the O—O antibonding π orbitals are filled. The O—O bond thus breaks as the released O atom simultaneously bridges over the As atom under consideration and a nearest-neighbor surface Ga; the other O atom at the same time strengthens its bonding with the As atom, forming the As=O dative bond.¹⁵ This leads to the oxygen bonding configuration we proposed in Sec. III C, which is shown on the right of Fig. 10(a). In Fig. 10(b) we show the top view of the proposed oxygen-bonding configuration. In the top view we recognize that there are two equivalent surface bonds which the released O atom from the peroxy zwitterion can attack. This ambivalent position of the released O atom from the peroxy zwitterion may lead to a random variation between 1 and 2 in the oxygen coordination number of surface Ga atoms. Since the chemical shift in Ga 3*d* induced by oxygen adsorption is not resolved, the randomness of the oxygen coordination of surface Ga is not inconsistent with the experimental results. The oxygen coordination number for surface As, however, is fixed in this proposed adsorption mechanism, which is consistent with the constant value of chemical shift in As 3*d* at various oxygen coverages.

In contrast to the above-proposed dissociation mechanism, if oxygen molecules dissociate at defect sites and then react at normal sites, the dissociated O atoms would be very reactive and would favor the formation of the Ga—O—As bond over the As=O bond⁴; in forming the Ga—O—As bonds, surface Ga—As bonds may be randomly attacked to cause random oxygen coordination of surface As at different oxygen coverages, which is inconsistent with the constant value of chemical shift in As 3*d*.

In summary, we have proposed that oxygen molecules dissociate on GaAs(110) through interacting with the As lone pairs of surface As. This proposal is motivated by (i) one class (perhaps the most important class) of defects on GaAs(110) which is found to be passivated before oxygen begins to adsorb on normal surface sites, and (ii) the constant oxygen coordination number of surface As at different oxygen coverages.

IV. RESULTS AND DISCUSSION OF OXYGEN ADSORPTION ON DISORDERED GaAs(110) SURFACES

In this section we present results of room-temperature oxygen adsorption on GaAs(110) sur-

faces disordered by inert ion (Ar^+) sputtering. Sputtering introduces both structural disorders (loss of LEED pattern) and compositional imperfection (loss of stoichiometry) to GaAs(110) surfaces. Oxygen adsorption on disordered surfaces tests the importance of the long-range order of the surface structure in the oxygen-adsorption processes, when compared to adsorption on cleaved surfaces.

Two samples have been studied: one *p*-type sample (sample *P3*, Figs. 11 and 15) studied with He I and He II radiation, and one *n*-type sample (sample *N6*, Figs. 12 and 13) studied with 100-eV synchrotron radiation. We will first describe the properties of the sputter-disordered surfaces, as deduced from the photoemission spectra of these surfaces (Sec. IV A). Oxygen-induced features in the photoemission spectra are analyzed in Sec. IV B. The oxygen-adsorption process on disordered GaAs(110) will be discussed in Sec. IV C.

A. The sputtered surface

The He I spectra obtained on sample *P3* are shown in Fig. 11. The sputtering (500-eV Ar^+ , 15

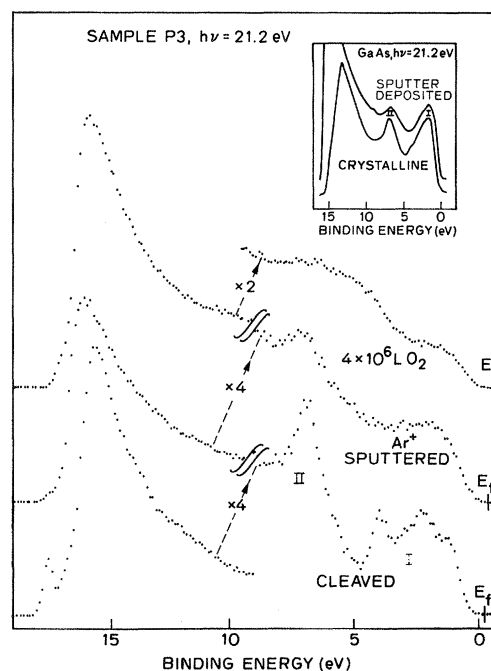


FIG. 11. He I spectra of clean, sputtered, and oxygen-exposed *p*-GaAs(110). The inset shows the He I spectra of crystalline and amorphous GaAs obtained by Shevchik *et al.* (Ref. 21).

min) had produced layers of well-disordered GaAs, as can be seen by comparing the smearing of the "fine" structures in the upper p -like band (in the 0–5-eV BE region, labeled I in Fig. 11) and the broadening of the s - p mixed band (peak II in Fig. 11, 6.9-eV BE). Similar, but to less degree, smearing of the valence-band features were observed in the He I spectrum of sputter-deposited GaAs (the upper curve in the inset of Fig. 11) obtained by Shevchik *et al.*²¹ The different degree of smearing could be due to a real difference in the properties of the sputter-disordered surface in our work and the sputter-deposited film studied by Shevchik *et al.* A high stoichiometry of the sputter-deposited film was reported by Shevchik *et al.*, whereas As deficiency is expected for the sputter-disordered surface (Fig. 12 to be discussed below).

The bottom curve Fig. 12 shows the Ga $3d$ and the As $3d$ levels of an n -type sample cleaved in vacuum and then sputtered with 1-keV Ar⁺ ion for 10 min. (The spectra for the cleaved surface was not obtained.) A comparison of the ratio of the areas under Ga $3d$ and As $3d$ of the sputtered surface to that of a cleaved surface (that of Fig. 1, for example) reveals that about ~22% As in a region near the surface were lost during sputtering (see Table III below for more discussion). However strong the As deficiency may be, no coagulation of Ga atoms into droplets occurs under the sputtering conditions used here. This is evidenced by (1) the lack of emission in the energy region above the valence-band maximum and below the Fermi level in the valence-band spectra of sputtered surfaces (Figs. 11, 13, and 15), and (2) the lack of chemical shift in the Ga $3d$ level toward the lower BE side (Fig. 12 and Fig. 15 to be discussed below). Thus, the majority of Ga atoms occupies tightly bonded tetrahedral sites even at the presence of a larger number of As deficiency. The As deficiency leaves behind simple As vacancies or sites with few of the four Ga–As bonds to a Ga

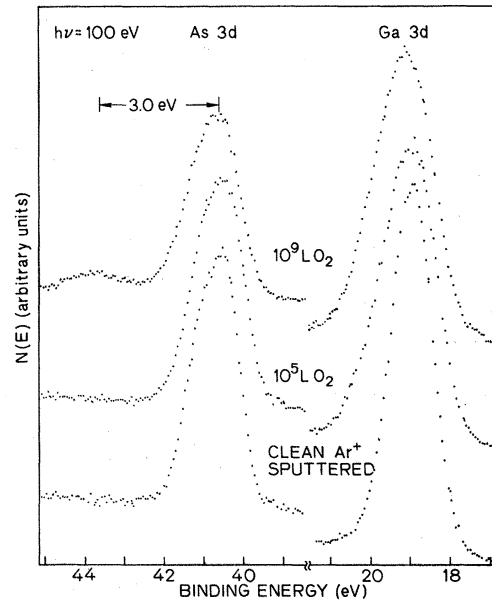


FIG. 12. Ga $3d$ and As $3d$ levels of clean and oxygen-exposed sputter-disordered GaAs(110). At the 10^5 -L exposure oxygen atoms are bonded to Ga only.

atom being replaced by Ga–Ga wrong bonds²¹ or both, such that a substantial amount of Ga atoms in the surface region are seeing other Ga atoms as nearest neighbors. This picture of the sputtered surfaces is important in understanding the oxygen adsorption process on disordered GaAs(110).

B. The DOVS of oxygen-adsorbed sputter-disordered surfaces

Figure 12 shows the effect of oxygen adsorption on the Ga $3d$ and the As $3d$ levels of a sputter-disordered surface; the spectra were taken with 100-eV synchrotron radiation. Exposing the disordered surface to 10^5 -L oxygen produced a significant amount of asymmetric broadening of the

TABLE III. Intensity changes in Ga, As, and O levels induced by oxygen adsorption on a sputter-disordered GaAs surface.

Treatment	Ga $3d$ (total)	Ga $3d$ (shifted)	As $3d$ (total)	As $3d$ (shifted)	O $2p$
cleaved	1.0	0	1.0	0	0
sputtered (Ar ⁺ , 1 keV, 10 min)	1.0	0	0.78	0	0
10^5 L O ₂	1.0	0.36	0.65	0	0.20
10^9 L O ₂	1.0	0.48	0.64	0.07	0.28

Ga 3d level toward the high-binding energy side ($\sim 36\%$, Table III, to be discussed below), whereas no change was induced in the As 3d level (center curve, Fig. 12). We therefore have a clear-cut case in which oxygen is bonded to Ga but not to As. Spectra of the O 2p level are presented in Fig. 13. With the 10^5 -L exposure, the spectrum represents oxygen bonded to Ga only. The oxygen-induced features in this spectrum are the broad peak at 5.3 eV and the shoulder at ~ 10.3 -eV peak. As oxygen exposure is increased to 10^9 -L, a small amount of shifted As 3d characteristic of oxygen bonding to As also appeared (top curve, Fig. 12), while the broadening in the Ga 3d level is further increased. Oxygen-induced features do not change significantly. We conclude that the 10^9 -L valence-band spectrum in Fig. 13 is dominated by that due to oxygen bonded to Ga.

The oxygen bonded to Ga atoms on disordered GaAs surfaces is in a form distinctly different from Ga_2O_3 . In Fig. 14 we compare the Ga 3d level and the O 2p level of the disordered surface exposed to 10^5 -L oxygen and those of a GaAs surface oxidized by oxygen plasma to Ga_2O_3 . The two spectra are plotted with the major oxygen peak aligned. The three features associated with Ga_2O_3

at 5.5-, 7.3-, and 9.7-eV BE (Ref. 12) are clearly seen in the top curve of Fig. 14. The 7.3-eV feature is missing in the spectrum of the disordered surface. Another distinction between the spectrum of oxygen adsorbed on disordered GaAs(110) and that of Ga_2O_3 is in the energy positions of the Ga 3d level. When the major oxygen peaks are aligned the Ga 3d levels in the two cases are separated by 1.7 eV. As indicated in Fig. 14, the vertical line drawn through the Ga 3d peak of the Ga_2O_3 spectrum intercepts little of the Ga 3d peak in the spectrum of oxygen adsorbed on disordered GaAs. In making the comparison in Fig. 14 we have suggested the use of an internal reference, namely, the separation between the nonbonding O 2p peak and the Ga 3d peak, to identify different oxygen bonding states. The separation between the Ga 3d peak and the oxygen peak in the lower curve of Fig. 14 is 13.6 ± 0.2 eV. The apparent peak position of the Ga 3d peak in the spectrum of the sputtered surface, however, is determined by the Ga 3d emission from Ga atoms not bonded to oxygen, because the surface is only partially covered with oxygen. The Ga 3d from Ga atoms bonded to oxygen is shifted to the high BE side of the substrate Ga 3d. The shift was not resolved in either

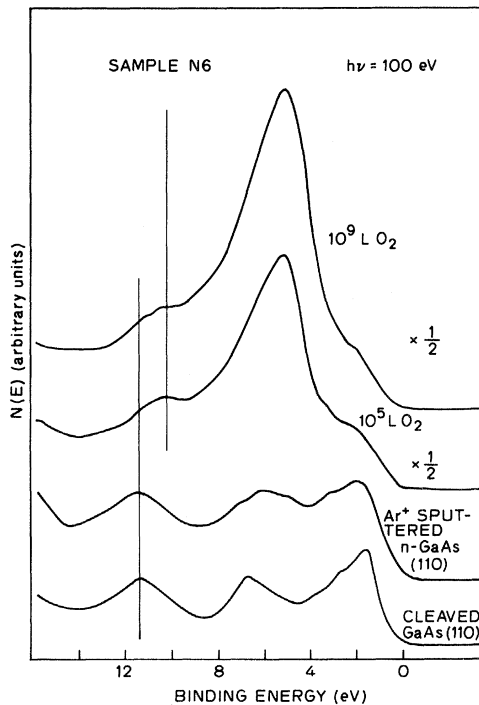


FIG. 13. Valence-band spectra of clean and oxygen-exposed sputter-disordered GaAs(110) measured at $h\nu = 100$ eV.

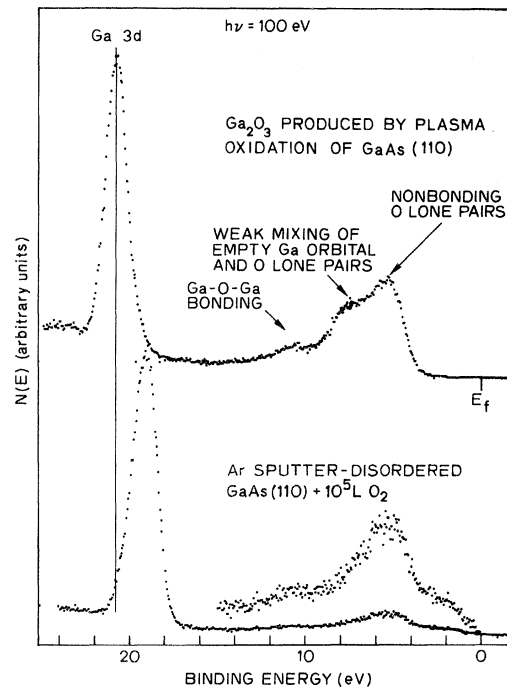


FIG. 14. Comparison of the Ga 3d level and the valence-band region of an oxygen-exposed sputtered GaAs(110) to those of Ga_2O_3 . Both spectra were obtained at $h\nu = 100$ eV.

Fig. 12 or Fig. 15. Curve fitting the broadened Ga 3d peak after oxygen adsorption with two clean Ga 3d components or taking the difference between the before and after adsorption Ga 3d spectra suggests the shift to be at most 0.8 eV. The separation between the Ga 3d peak and the oxygen peak for oxygen adsorbed on disordered GaAs is therefore 14.4 ± 0.2 eV. The corresponding separation of Ga₂O₃ is 15.3 ± 0.2 eV. The 0.9-eV difference unambiguously distinguishes the two forms of O—Ga bonding. A parallel situation has been reported for O—Al bonding: The separation between the Al 2p peak and the oxygen peak is 1.3 eV smaller for a well-defined chemisorption phase than that for Al₂O₃.²³ This parallel with the better studied Al—O system seems to support the appropriateness of assigning one form of O—Ga bonding as a chemisorption phase and the other form as bulk oxide.

An interpretation of the spectrum of oxygen adsorbed on disordered GaAs surfaces, on the other hand, can be offered by noticing both its similarities and differences with the spectrum of Ga₂O₃. As discussed in detail in Ref. 12, the three features in the spectrum of Ga₂O₃ have their origins as the nonbonding oxygen lone pair (5.5-eV BE), the donorlike bonding between an oxygen lone pair and an empty Ga orbital (7.3-eV BE), and the Ga—O—Ga bonding band (~ 9.7 -eV BE). The spectrum of O—Ga on disorder GaAs(110) is essentially the same Ga₂O₃ spectrum with the donorlike bonding band missing. As pointed out in Ref. 12, the donorlike bonding between oxygen lone pairs and empty Ga orbitals can be viewed either as the results or as the cause of the high coordination number in Ga₂O₃. We therefore simply interpret the spectrum of the O—Ga bonding on sputter-disordered GaAs(110) as due to isolated Ga—O—Ga units.

A spectrum similar to that of isolated Ga—O—Ga units on disordered GaAs(110) has been observed for oxygen adsorbed on Ga metal at 70 K by Schmeisser *et al.*²² This is seen in Fig. 15, where we have displayed the HeII spectra of the surfaces of Fig. 11 and the spectrum of oxygen adsorbed on Ga metal at 70 K (the top curve, reproduced from the work of Schmeisser *et al.*²²). The peak at 5.3-eV BE and the shoulder centered at ~ 10.3 -eV BE developed after the 4×10^6 -L exposure on this sputter-disordered GaAs(110) are the same as those shown in Fig. 13, and they also appear in the spectrum of oxygen adsorbed on Ga metal at 70 K (top curve, Fig. 15). Schmeisser

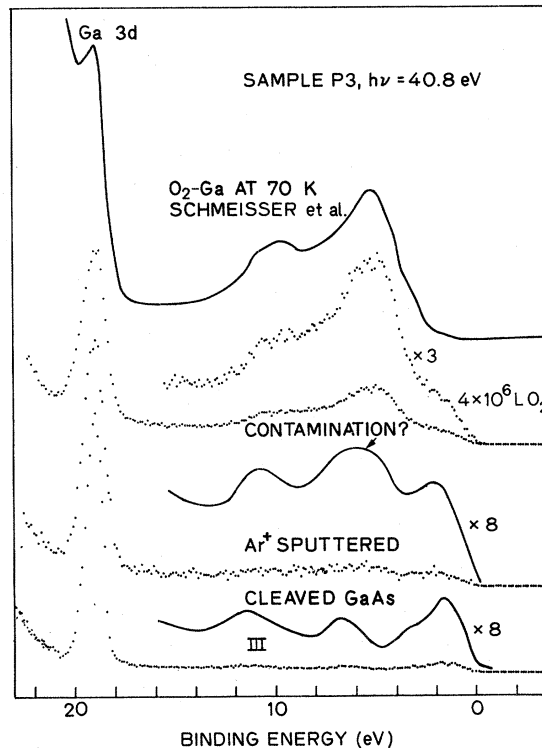


FIG. 15. HeI spectra of the surfaces of Fig. 11. The top spectrum is due to oxygen chemisorbed on Ga metal at 70 K (Ref. 22). Notice the similarity between the top two spectra.

et al. interpreted the spectrum to be due to molecularly chemisorbed oxygen, motivated by its evolution from physisorbed oxygen molecules at low temperatures (~ 4 K). The spectrum of the chemisorbed oxygen, however, does not show strong reminiscence of the multiple splittings characteristic of the O—O bonding. Therefore, we believe the spectrum observed by Schmeisser *et al.* can also be explained by dissociated oxygen in the Ga—O—Ga bonding. The observation of the same Ga—O—Ga chemisorption form on both the crystalline Ga surface and the sputter-disordered GaAs(110) surface is rather intriguing. Exposure of Ga to oxygen at room temperature always results in the formation of Ga₂O₃.¹² This is expected because Ga is a liquid at room temperature; the condition is comparable to high-temperature oxidation of Al where Al₂O₃ is always formed.²³ The high mobility of Ga at room temperature does not allow any intermediate state but the most stable Ga₂O₃ to form. At low temperature Ga metal is in crystalline form, the low mobility and the close packing of Ga may stabilize the chemisorption phase. As discussed in Sec. IV A, the majority of Ga atoms occupies tightly bonded tetrahedral sites

even at the presence of a large As deficiency, rather than forming Ga clusters. The tight binding of the Ga atoms may present an activation barrier against the direct formation of Ga_2O_3 .

Since the sputter-disordered surface is deficient of As, the preferential bonding of oxygen to Ga is not surprising as it is expected from elemental thermodynamics. The absence of the formation of Ga_2O_3 , however, is rather intriguing. Since even on a disordered GaAs surface with a large number of Ga atoms seeing Ga atoms as next-nearest neighbors the formation of Ga_2O_3 is strongly prohibited, it is very unlikely that room-temperature adsorption of oxygen on cleaved, ordered GaAs(110) surface can result Ga_2O_3 at the initial stage.

The chemisorbed oxygen on the disordered surface is also different from the oxygen adsorbed at the normal sites on cleaved, ordered GaAs at room temperature (Secs. III B and III C). In Fig. 16 we compare the He II spectra of a cleaved, ordered GaAs(110) surface exposed to 10^8 -L oxygen and a disordered surface exposed to 4×10^6 -L oxygen (sample P3, Fig. 15). The Ga 3d peaks of the two

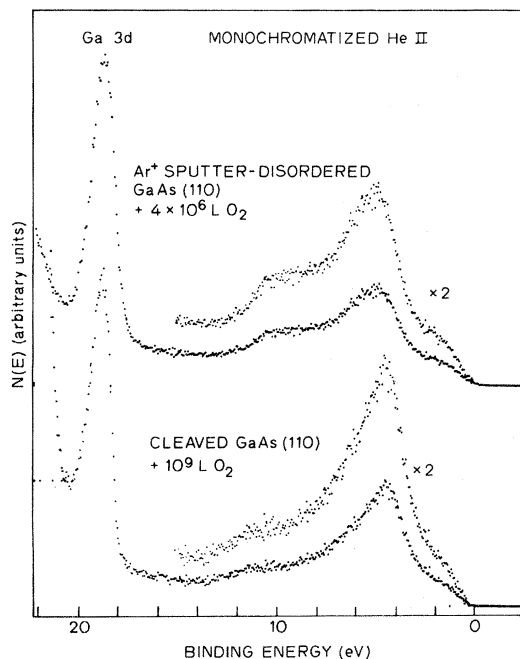


FIG. 16. Comparison of the Ga 3d level and the valence-band region of oxygen-exposed sputtered GaAs(110) to those of oxygen-exposed cleaved GaAs(110). Both spectra were taken at $h\nu=40.8$ eV (He II).

cases are aligned. The major oxygen peak of the ordered surface is 4.5 ± 0.2 eV below VBM, whereas that for the disordered surface is 5.3 ± 0.2 eV below VBM. The relatively pronounced 10.3-eV shoulder appearing in the spectrum of the disordered surface is not pronounced in the spectrum of the ordered surface. The small intensity which exists in the region near 10.3-eV BE in the spectrum of the ordered surface is due to the small amount of Ga—O—Ga bonding at defect sites of the GaAs(110) surface (see Sec. III D) above). We thus conclude that the oxygen adsorbed at the normal sites on cleaved, ordered GaAs(110) surfaces does not occur in the form of Ga—O—Ga bonding.

C. The adsorption process on disordered surfaces

Information revealing a different adsorption process on disordered GaAs surfaces, based on the results obtained on sample N6, are summarized in Table III. Again, intensities of different peaks of each treatment are normalized to the total intensity of Ga 3d level. As atoms in the surface layer contribute about 50% of the total emission of the As 3d level when excited by a 100-eV photon (Table I, Sec. III B). The 22% loss of As created by sputtering is equivalent to one-half of the surface layer. This deficiency of As, however, is more likely to be distributed over a few layers below the surface, because the 1-keV ion is capable of producing damages a few lattice layers deep.²⁴ The value of $\frac{1}{2}$ can be taken as an upper limit of the deficiency of As in the surface layer. Perhaps the most interesting number in Table III is the decrease in the As 3d intensity after the 10^5 -L oxygen exposure. The decrease of 0.13 corresponds to approximately one-quarter of the As in the surface layer of a stoichiometric GaAs(110) surface. If the surface layer was one-half As deficient before the oxygen adsorption, the decrease is even more significant. Several possibilities can account for this decrease: (i) a shift of the photoelectron escape-depth minimum to lower kinetic energy by oxygen adsorption, so more Ga atoms are sampled after oxygen adsorption, (ii) preferential attenuation of the As 3d signal by the oxygen overlayer, and (iii) depletion of As atoms from the surface layer during the adsorption process.

Possibility (i) is not favored because we did not observe an increase in the absolute intensity of the Ga 3d level after oxygen adsorption; instead, we

observed an $\sim 12\%$ decrease in the absolute intensity of the Ga $3d$ level after oxygen exposure, which is reasonable with the attenuation by the 0.3 monolayer oxygen. Possibility (ii) is unlikely because oxygen is bonded to Ga only. Two possible channels exist for depleting As [possibility (iii) above] during the oxygen-adsorption process:

(i) One is the formation of As_2O_3 with loosely bonded As in the disordered surface layer and the subsequent desorption of As_2O_3 by the exothermic oxidation energy.

(ii) The other is that the formation of the Ga—O—Ga bonding requires Ga—Ga nearest neighbors, hence some As in Ga-rich regions (i.e., regions containing a substantial amount of Ga—Ga nearest neighbors because of As vacancies or Ga—Ga wrong bonds or both; (see Sec. IV A above for more rigorous description) are removed (as As_2 or As_4) before O—Ga bonding commences; the energy needed for the removal of As can be supplied by the exothermic adsorption energy from initial O—Ga bondings in the surrounding Ga-rich region.

We could not distinguish between the two possibilities from the results discussed so far. The important thing to point out here is that the depletion of As in the adsorption process on disordered surfaces forms a striking contrast to the adsorption on ordered surfaces. The oxygen uptake on the disordered surface is faster compared to that on ordered surfaces only initially, i.e., only during the period when all adsorbed oxygen are bonded to Ga. At 10^9 -L exposure, the total amount of oxygen adsorbed is comparable to that adsorbed on ordered surfaces using the same oxygen exposure (compare with Table I). We also notice the increasing oxygen exposure from 10^5 to 10^9 L did not introduce further loss of As. It appears that after the 10^9 -L exposure some oxygen was adsorbed on a number of "normal" surface sites [sites retaining the local bonding structure of the ordered GaAs(110)], because chemical shift in the As $3d$ level characteristic of oxygen chemisorbed on ordered surfaces had emerged. We can tentatively separate the oxygen adsorption process on disordered GaAs surfaces into two steps. Oxygen is first adsorbed at sites with Ga—Ga nearest neighbors on the disordered surface and this adsorption quickly slows down as the available sites for such adsorption decreases. Oxygen atoms are then adsorbed on patches of normal GaAs sites at a rate no faster than that on ordered GaAs(110) surfaces. We see no evidence

here that the gross disorders introduced by sputtering speed up the formation of bulk oxides (Ga_2O_3 , As_2O_3).

As mentioned in Sec. III E, Mark *et al.*²⁰ have suggested that the oxidation of GaAs(110) commences on residual defect sites and produces additional disorder owing to the release of exothermic adsorption energy so that, as the oxidation progresses, the entire surface becomes disordered. If oxygen adsorbs only on defect sites, one would expect to observe the same state of oxygen, possibly Ga_2O_3 and As_2O_3 , being formed on ordered and disordered surfaces. The absence of Ga_2O_3 and the two-site adsorption process on the disordered surfaces, therefore, argue against the adsorption process proposed by Mark *et al.*

V. RESULTS AND DISCUSSION OF EFFECTS OF HEAT TREATMENTS OF OXYGEN-COVERED SURFACES

In this section we present results of thermal annealing experiments. The annealing was carried out on (cleaved, unspattered) surfaces which were adsorbed with oxygen to various coverages at room temperature. Knowledge of the effects of annealing reveals the stability of the room-temperature O-GaAs(110) bonding and thus provides additional insights into the room-temperature interaction with GaAs(110).

A basic effect of annealing is the transfer of oxygen from As to Ga (to form Ga_2O_3 , the discussion of which will be deferred until describing the valence-band spectra) and the loss of those As atoms which are released from the arsenic-oxygen bonding from the surface. In panels (a) and (b) of Fig. 17, we show, respectively, the As $3d$ and Ga $3d$ core levels of GaAs(110) surface exposed to 10^{10} L O_2 ($\Theta \approx 0.6$) at room temperature and then annealed to 370°C for approximately 30 min. The spectra are normalized to have equal height for the unshifted As $3d$ peaks. The sharp decrease (by a factor of ~ 6) in the intensity of the shifted As $3d$ [Fig. 17(a)] and the increase in the broadening toward high BE of the Ga $3d$ [Fig. 17(b)] are clear. Also apparent is the increase in the ratio of total intensity of Ga $3d$ to As $3d$. (This ratio is not affected by the normalization.) The decrease in the intensity of the shifted As $3d$ approximately equals the decrease in the total intensity of As $3d$. Thus, only those surface As atoms bonded to oxygen after room-temperature adsorption are lost from the surface during annealing. On the other hand,

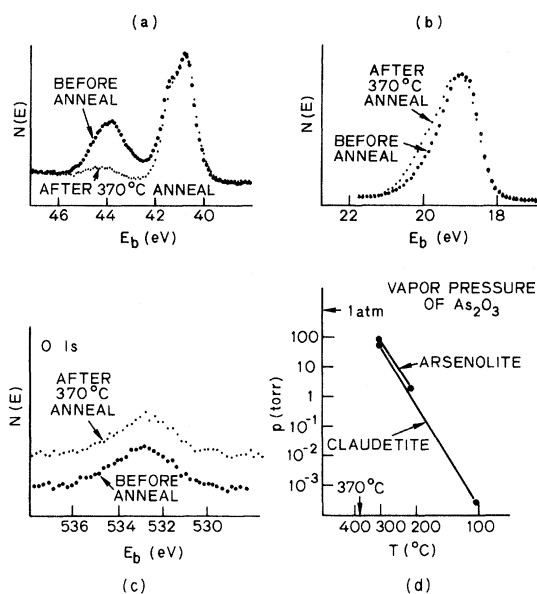


FIG. 17. Effect of annealing of a room-temperature oxygen-exposed surface at 370°C for 30 min. Transfer of oxygen from As (a) to Ga (b) without loss of oxygen (c) has been observed. However, As originally bonded to oxygen leaves the surface after releasing its oxygen to Ga. For reference, (d) shows the temperature dependence of the vapor pressure of the two forms of As_2O_3 .

the O 1s intensity is seen in Fig. 17(c) to show no detectable change after annealing, indicating that no desorption of oxygen has occurred during annealing.

In Fig. 18 we show the effects of annealing to 250°C for 30 min on another surface exposed to $\sim 10^{11}$ L O_2 ($\Theta \approx 0.75$). The decrease in the intensity of the shifted As 3d and the increase in the broadening toward high BE side of the Ga 3d after annealing is much less pronounced than that caused by the 350°C anneal (Fig. 17). This suggests that the arsenic-oxygen bonding formed by room-temperature adsorption of oxygen on GaAs(110) is rather stable at 250°C. This is consistent with the presence of As=O bond (Sec. III C), because the As=O bond in As_2O_3 becomes unstable only at temperatures above 315°C.²⁵

On the other hand, the results in Figs. 17 and 18 are inconsistent with the presence of As_2O_3 after room-temperature adsorption. If the chemically shifted As 3d were to be interpreted as due to As_2O_3 , there would be two competing channels to remove As_2O_3 at elevated temperatures: one is the evaporation of As_2O_3 and the other is the reaction of As_2O_3 with substrate GaAs to form Ga_2O_3 . In Fig. 17(d) we show the variation of vapor pressure

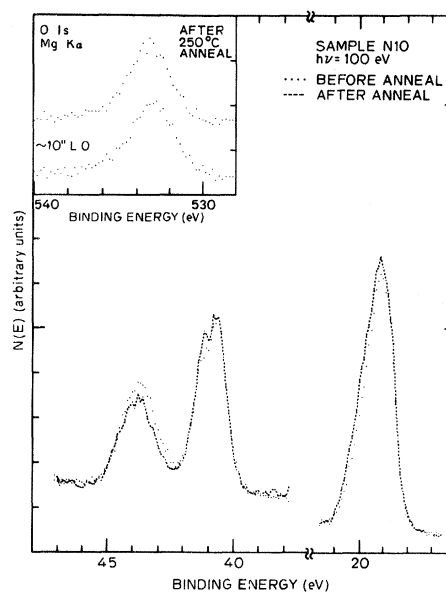


FIG. 18. Effect of annealing of a room-temperature oxygen-exposed surface at 250°C for 30 min. The changes in the As 3d and the Ga 3d are much less pronounced than that observed in Fig. 17.

with temperature of the two crystalline forms of As_2O_3 .²⁶ These curves indicate the high volatility of As_2O_3 at room temperature and above. In particular, by using the extrapolated values of vapor pressure at 250 and 370°C, and by using an unusually low evaporation coefficient of $\sim 10^{-7}$,²⁷ evaporation rates of $\sim 1 \times 10^{14}$ and 7.5×10^{16} molecules/cm² sec are found at 250 and 370°C, respectively. With these evaporation rates, it requires only 0.1 sec to evaporate a monolayer (10^{15} molecules/cm²) of As_2O_3 at 370°C and 10 sec at 250°C. The absence of desorption of oxygen is possible only if the reaction of As_2O_3 with GaAs to form Ga_2O_3 is much faster than the evaporation of As_2O_3 and the shifted As 3d disappears completely in 0.1–10 sec after annealing. However, the chemically shifted As 3d did not disappear completely (Figs. 17 and 18) after holding the sample at either 250 and 370°C for 30 min. The shifted As 3d remained after the 250°C anneal is about 90% of the original intensity and that remained after the 370°C anneal is about one-sixth of the original intensity. It is hard to explain why such a significant amount of As_2O_3 which escaped transforming into Ga_2O_3 by heating could stay on the surface without being evaporated away. The interpretation of the chemical shift in As 3d as due to As_2O_3 is thus considered highly improbable.

The end product of the annealing process can be

determined by combining results from the valence-band spectra and the results from the core-level spectra described above. In Figs. 19 and 20, we show He II spectra of a GaAs(110) surface subjected to programmed temperature treatments (in which the sample was raised to successively high temperatures) after the room-temperature exposure. The temperature increment is 50°C and the annealing time at each temperature was ~ 10 min. Different changes induced by annealing in the valence spectra are seen in the low-temperature range (50 – 200°C) and the high-temperature range (250 – 450°C). Hence, they are separately displayed in Figs. 19 and 20. The major change produced by annealing in Fig. 19 is the removal of intensity from the region at ~ 10.3 -eV BE. This effect is noticeable at 50°C and is about complete at 200°C . The major effect of annealing at higher temperatures, as seen in Fig. 20, is the development of a new feature in the 8 – 10 -eV BE region. This effect is noticeable at 250°C and becomes very pronounced at 450°C . At 480°C all oxygen desorbs (labeled "heat-cleaned" in Fig. 20).

The annealing effects in the DOVS' are more closely examined in Fig. 21. In panel (a) the 200°C spectrum is subtracted from the room-temperature spectrum, and the difference is displayed

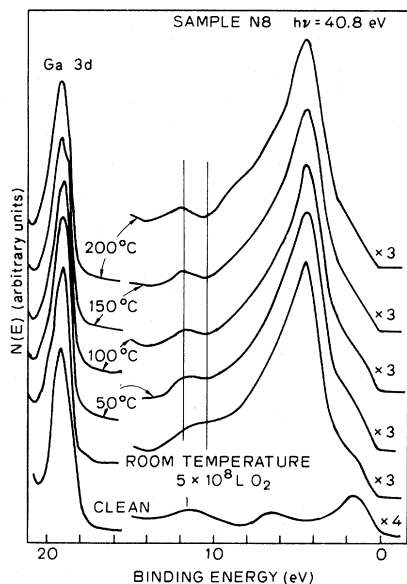


FIG. 19. Effects of annealing of a room-temperature oxygen-exposed n -GaAs(110) in the temperature range of 50 – 200°C . The sample was held at each temperature for 10 min. Spectra were taken at $h\nu=40.8$ eV (He II). The bottom curve is the spectrum of the clean surface.

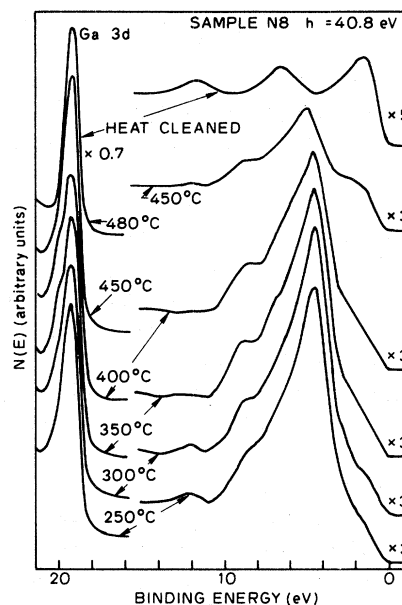


FIG. 20. Effects of annealing of the surface of Fig. 19 in the temperature range 250 – 450°C . The sample was held at each temperature for 10 min. The top spectrum shows the surface being heat cleaned after heating at 480°C .

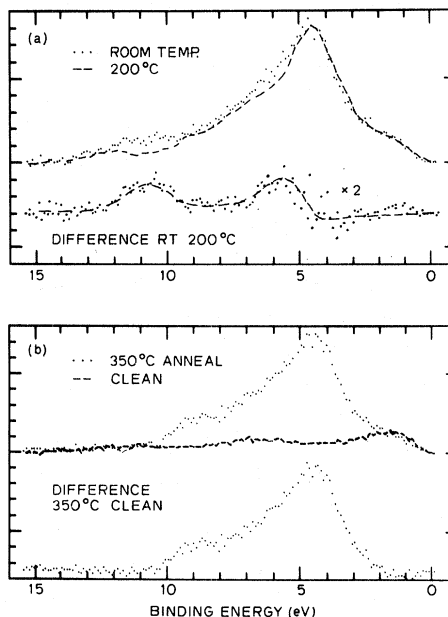


FIG. 21. (a) Difference curve (the bottom curve) obtained by subtracting the 200°C (dashed) from the room-temperature spectrum (dotted). It shows that the oxygen adsorbed at defect sites of GaAs(110) desorbs at $\sim 200^\circ\text{C}$. (b) Difference curve (bottom curve) between the 350°C spectrum (dotted) and the clean-surface spectrum (dashed). The resemblance of the difference curve to the spectrum of Ga_2O_3 (Fig. 7) indicates the formation of Ga_2O_3 by annealing to temperature $\geq 300^\circ\text{C}$.

at the bottom. The difference is noisy, but two features at ~ 5.5 - and 10.5 -eV BE are discernable. These binding energies are the same as those found for the low-coverage state oxygen in Sec. III D. Thus, oxygen adsorbed at the defect sites of GaAs(110) desorb at temperatures between 150 and 200°C. The binding energies of the two features in the difference curve of Fig. 21(a) are also the same as those of the Ga—O—Ga bonding complexes found on the sputter-disordered GaAs surfaces (Sec. IV). We therefore propose the low-coverage state of oxygen to be in the Ga—O—Ga bonding form. This proposal is consistent with its low desorption temperature, because Ga₂O, which is essentially an isolated Ga—O—Ga bonding unit, is known to be highly volatile.

In panel (b) of Fig. 21 we have obtained the difference curve between the 350°C spectrum and the clean spectrum. The difference curve bears clear resemblance to the DOVS of Ga₂O₃ (Fig. 6, Sec. III B). Hence the new feature developed in the 8–10-eV BE region observed in Fig. 20 is due to the formation of Ga₂O₃. Figure 20 also indicates that the formation of Ga₂O₃ is significant only at temperature above 300°C, which is consistent with the conclusion drawn from comparing Figs. 17 and 18.

It is also interesting to notice the difference in binding energies of the features in panel (a) and those of the difference curve in panel (b). The difference is consistent (although different in detail) with the comparison made in Fig. 14 between Ga—O—Ga and Ga₂O₃.

In Fig. 20 an additional change in the DOVS is seen to have occurred at 450°C: The nonbonding oxygen peak shifted to higher binding energy. We also notice that a considerable amount of oxygen desorbs at 450°C such that the oxygen coverage after the 450°C anneal is low. The same shift in oxygen nonbonding peak is also produced by going directly to an elevated annealing temperature on a low-oxygen coverage surface. In Fig. 22 we show sample P2 exposed to 10^7 L O₂ ($\Theta \approx 0.15$) at room temperature and then annealed at 350°C for 30 min. Since low oxygen coverage is a common factor in the two cases, we suggest that the 450°C spectrum in Fig. 20 or the after-anneal spectrum in Fig. 22 represents DOVS of oxygen-deficient gallium oxide, i.e., Ga₂O_{3-x}, with the value of x between 1 and 2. At high temperature (450–480°C), the desorption is likely to occur through the reduction reaction

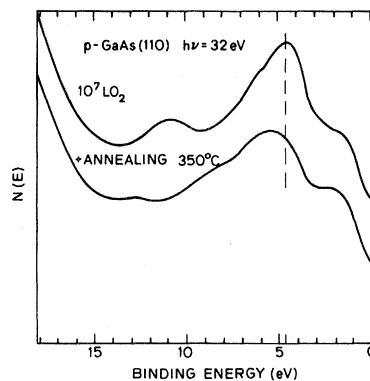
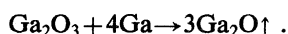


FIG. 22. Annealing of a low-oxygen coverage surface to 350°C. The changes seen here are the same as that observed between annealing at 400 and 450°C of a high-oxygen coverage surface (Fig. 20). Spectra were taken at $h\nu = 32$ eV.

Before complete desorption of oxygen occurs, some oxide intermediate between Ga₂O₃ and Ga₂O, which is less volatile than Ga₂O, may remain on the surface. For surfaces initially covered with a small amount of oxygen, annealing brings nearby oxygen to form Ga₂O_{3-x}, but Ga₂O₃ cannot be formed because of the deficiency of oxygen at a particular site on the surface. This result of annealing of low oxygen coverage surface is in fact an evidence against the picture that oxygen adsorb in patches or islands on GaAs(110).

When the heat-cleaned surface of sample N8 is re-exposed to oxygen, the same Ga—O—Ga state as that observed on sputter-disordered surface is found. This is shown in Fig. 23, where two oxygen features at 5.3- and at 10.3-eV BE are clearly seen. The amount of oxygen adsorbed in the Ga—O—Ga form on heat-cleaned surfaces is smaller than that found on sputter-disordered surfaces but is far higher than that found on cleaved surfaces. Since heating is expected to produce an As deficiency in the surface region, the results shown in Fig. 23 again reinforce the importance of removing As before forming the Ga—O—Ga bonding units.

In all the above annealing experiments, temperature was slowly (≤ 5 °C/min) brought up to the annealing temperature and then kept at that temperature for the indicated time. Only slight increases in the background pressure were detected during annealing. On two other surfaces, where we have attempted to heat to higher temperatures with faster rates (≥ 20 °C/min for $T \geq 300$ °C), heatings were terminated immediately after sharp pressure rises

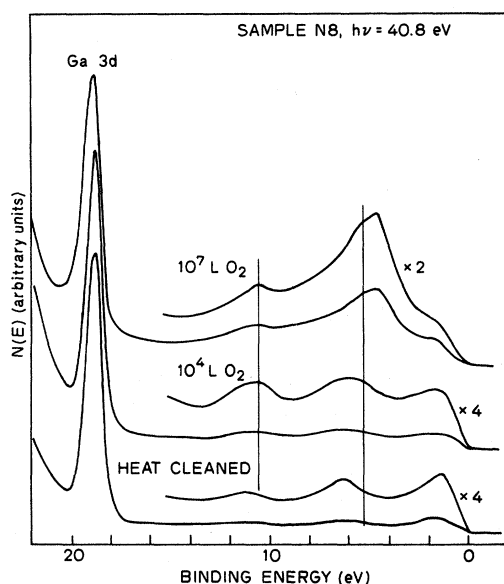


FIG. 23. Re-exposure of the heat-cleaned surface of Fig. 20 to oxygen. Spectra were taken at $h\nu=40.8$ eV.

were detected. Although no mass-spectrometric measurement was done, the photoelectron spectroscopic measurements of the resulting surfaces indicate that, as will be discussed below, the sharp pressure rises could well be correlated to desorption of As and oxygen from the sample surfaces, and did not correspond to any outgassing of other surfaces in the vacuum chamber. In one case, substantial transformation of oxygen from As to Ga was also observed in addition to the desorption of As and oxygen. Such complication reflects the lack of accurate control in the heating rate in our experiments. Better control of the heating rate and a systematic search for effects due to different heating rates should be of great interest in the future. However, in another case, little transformation of oxygen from As to Ga was observed to accompany the desorption. Results from this latter case clearly contrast the results from the annealing experiment we just discussed, hence they will be presented below.

In Fig. 24 we show core-level spectra of a GaAs(110) surface exposed to 10^9 L O_2 ($\Theta \approx 0.5$) at room temperature and then heated at a relatively rapid rate to 430°C . The curve with heavy dots in Fig. 24 shows the normally observed chemically shifted As 3d and the broadening in the Ga 3d after room-temperature adsorption. The spectrum taken after heating to 430°C shows complete disappearance of the shifted As 3d. But in contrast to the

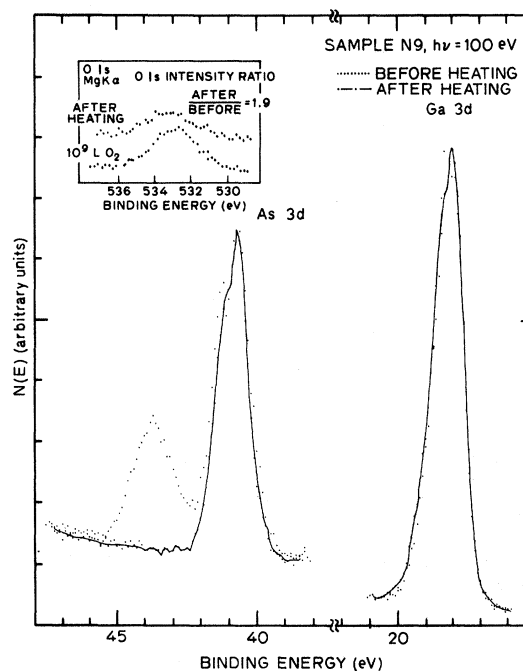


FIG. 24. Effect of fast heating of a room-temperature oxygen-exposed surface to $\sim 430^\circ\text{C}$. In contrast to the effect of annealing at 370 and 250°C (Figs. 17 and 18), a decrease of about a factor of 2 is seen in the O 1s intensity (inset) and the shifted As 3d disappeared without appreciable change in either the unshifted As 3d or the Ga 3d.

results shown in Fig. 17, there is only a barely detectable increase in the broadening in the Ga 3d. The O 1s intensity, as shown in the inset of Fig. 24, decreased by a factor close to 2. The total intensity of As 3d decreased by approximately 25% which is equal to the percent-shifted As 3d before heating. The decrease in intensity of O 1s and As 3d in conjunction with the pressure burst detected immediately prior to the termination of heating are strong indications of desorption of both oxygen and As from the sample surface. The slight increase in the broadening in Ga 3d and the small deviation of the oxygen intensity ratio from two is attributed to a small amount of oxygen transformed from As to Ga before the termination of the heating.

The result of Fig. 24 is not inconsistent with the oxygen-bonding model we proposed in Sec. III C. In Fig. 25 we show on the left the proposed oxygen bonding in a zig-zag chain in the (110) surface. After fast heating to 430°C , the As=O units desorb from the surface as AsO molecules, and oxygen atoms originally bridged over Ga and As now

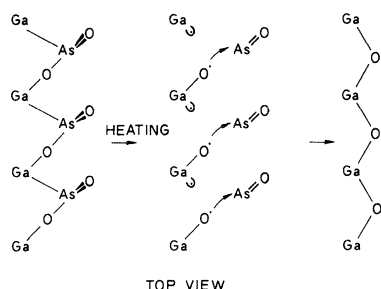


FIG. 25. Changes of the proposed O-GaAs(110) bonding after fast heating.

bridge over two neighboring Ga, as displayed on the right of Fig. 25. The transformation shown in Fig. 25 makes the number of chemically affected Ga atoms unchanged after heating, and hence gives little change in the amount of broadening in Ga 3*d* after heating. The value of a chemical shift in Ga 3*d* however, should increase after heating, because each Ga bonds to one oxygen before heating and bonds to two oxygens after heating. This increase in the value of chemical shift may be small, because Ga atoms are required to supply more charges to O in Ga—O—As bridges than in Ga—O—Ga bridges. The increased oxygen coordination number and the decreased charge transfer per oxygen atom compensate each other to give a small net increase in the shift in Ga 3*d*, which may well escape our detection. Inclusion of valence-band spectra in future studies of heating rate dependent effects may give more unambiguous information about the end product of such fast heating. It is essential, however, to point out here that the oxygen coordination of Ga atom in the end product has to be higher than that in isolated Ga—O—Ga in order to explain the low volatility of the oxygen that survived the fast heating.

VI. SUMMARY

In summary we have made detailed analyses of the DOVS of oxygen-adsorbed, cleaved GaAs(110). Through the coverage dependence of the DOVS, two different forms of oxygen have been identified. Adsorption in the first form saturates at low coverage (~ 0.01 monolayer), and is suggested to occur at defect sites with As deficiency in the form of Ga—O—Ga. This first form of oxygen desorbs at $\sim 150^\circ\text{C}$, which is further support for the proposal that this form is in a bonding configuration closely resembling the highly volatile species Ga₂O.

Adsorption in the second form emerges after the saturation of first form, and produces a well-re-

solved shift in the As 3*d* ($\Delta E = 3.0$ eV) and broadening in the Ga 3*d*. The second form contains both nonbridging oxygen (As=O) and bridging oxygen (Ga—O—Ga), and is suggested to be in a Ga—O—As=O unit (Fig. 8). This suggested model is based on the following:

(i) The detailed interpretation of the DOVS of O-GaAs(110); in particular, the interpretation has been substantiated by the comparison with the experimental DOVS's of As₂O₃ and Ga₂O₃ (Sec. III C).

(ii) The stability of the arsenic-oxygen bonding under thermal annealing, which has been found to be consistent with the known stability of the As=O bond (Sec. V).

(iii) The constant chemical shift in the As 3*d* at oxygen coverages below one monolayer, which is consistent with the fixed oxygen coordination of As in this model.

(iv) The small shift in the Ga 3*d* at oxygen coverages below one monolayer, which is consistent with the low oxygen coordination number of Ga in this model.

(v) The successful explanation of the dissociation of oxygen molecules without invoking the dissociation at defect sites (Sec. III E).

Adsorption of oxygen on sputter-disordered Ga-rich GaAs(110) surfaces has been found to proceed in the same two-stage process as that found on ordered GaAs(110), only the relative concentration of the two forms of oxygen are reversed in the two cases according to the relative concentration of defect sites and normal sites on the two surfaces. This suggests that the adsorption on defect sites and the adsorption on normal sites are independent of each other. The picture that adsorption nucleates at defect sites and propagates through adsorption-induced defect sites does not appear to be appropriate for the room-temperature adsorption of oxygen on GaAs(110).

On either ordered or disordered surfaces, direct formation of Ga₂O₃ is not possible due to the activation barrier to bring Ga atoms together. The possibility of the formation of As₂O₃ by room-temperature adsorption of oxygen on GaAs(110) has also been definitively ruled out by the annealing experiments. The picture that room-temperature adsorption of oxygen on GaAs(110) produces islands of Ga₂O₃ and As₂O₃ is therefore considered inappropriate.

This work has demonstrated that much critical information can be obtained from careful examination of the DOVS's. It is therefore hoped that further theoretical calculations will be carried on to

allow more definitive interpretations of the DOVS's.

ACKNOWLEDGMENTS

We are grateful to Dr. D. Schmeisser for making his results available to us prior to publication. Valuable discussion with Professor W. Monch and Professor W. A. Harrison is gratefully acknowledged. We also want to thank the Stanford Tube Laboratory for excellent technical assistance, especially Jack MacGowan and Ron Morris. This work was supported by the Office of Naval Research under Contract No. N00014-75-0289 and by the Advanced Research Projects Agency of the Department of Defense under Contract No. N00014-79-C-0072. The experiments were performed at the Stanford Synchrotron Laboratory which is supported by the National Science Foundation under Grant No. DMR77-27489 in cooperation with the Stanford Linear Accelerator Center and the Department of Energy.

APPENDIX: CALCULATION OF THE N - B SPLITTINGS

In this appendix we give some details of the simple LCAO calculations which were used to obtain the N - B splittings of Sec. III C. The values of atomic levels used are $E(\text{As } 4s) = -17.33$ eV, $E(\text{As } 4p) = -7.91$ eV, $E(\text{Ga } 4s) = -11.37$ eV, $E(\text{Ga } 4p) = -4.90$ eV, and $E(\text{O } 2p) = -14.13$ eV. The values of matrix elements used are $V_{sp} = 14.02/d^2$ eV for that between s and p orbitals,

and $V_{pp} = 24.69/d^2$ eV for that between p orbitals, where d is the bond length in Å. The bond lengths used are $d = 1.62$ Å for the As=O bond, and $d = 1.8$ Å for As=O and Ga—O bonds.

For configuration I we have considered the As lone pair on the As atom to be purely s -like. Bonding of oxygen to this lone pair gives an N - B splitting of 3.91 eV. The donorlike bonding between the oxygen lone pair and the empty As $4d$ orbital lowers the oxygen lone pair in energy by ~ 0.55 eV.¹⁵ Hence the net N - B splitting entered for configuration I is 3.36 eV. For configuration II we have considered the interactions between O $2p$ and the Ga sp^3 and As sp^3 hybrids.

For simplicity in making comparisons, we have chosen the $X-O-X'$ angle to be 125° for configurations III, IV, and V. Small variations around this angle change the splitting between the σ and the π components rapidly but not the center of gravity of these two components. In considering the As—O—As bonding we have assumed the p^3 configuration for As, whereas we have assumed the p^3 configuration for Ga—O—Ga bonding. Such assumptions are justified by the bonding angles found in As₂O₃ and Ga₂O₃. For similar reasons, we have retained the p^3 configuration of the backgrounds of an As atom in a relaxed GaAs(110) surface when considering the Ga—O—As bridge (configuration IV). There are many variations of bond angles and hybridizations that can be considered, but those variations do not change the qualitative trend in the N - B splittings stated in the text (Sec. III C).

¹E. J. Mele and J. D. Joannopoulos, Phys. Rev. B **19**, 6999 (1978); Phys. Rev. Lett. **40**, 341 (1978); J. Vac. Sci. Technol. **15**, 1287 (1978).
²P. W. Chye, C. Y. Su, I. Lindau, P. R. Skeath, and W. E. Spicer, J. Vac. Sci. Technol. **26**, 1191 (1979).
³C. R. Brundle and D. Seybold, J. Vac. Sci. Technol. **16**, 1186 (1979).
⁴J. J. Barton, W. A. Goddard III, and T. C. McGill, J. Vac. Sci. Technol. **16**, 1178 (1979).
⁵P. Pianetta, I. Lindau, C. M. Garner, and W. E. Spicer, Phys. Rev. B **18**, 2792 (1978); Phys. Rev. Lett. **35**, 780 (1975); **37**, 1166 (1976).
⁶A. Kahn, D. Kanani, P. Mark, P. W. Chye, C. Y. Su, I. Lindau, and W. E. Spicer, Surf. Sci. **87**, 325 (1979).
⁷P. Pianetta, I. Lindau, P. E. Gregory, C. M. Garner, and W. E. Spicer, Surf. Sci. **72**, 298 (1978).
⁸R. Ludeke, Solid State Commun. **21**, 815 (1977).
⁹W. Ranke and J. Jacobi, Surf. Sci. **81**, 504 (1979).
¹⁰S. Doniach, I. Lindau, W. E. Spicer, and H. Winick, J.

Vac. Sci. Technol. **12**, 1123 (1975).
¹¹D. E. Eastman, T.-C. Chiang, P. Heiman, and F. J. Himpsel, Phys. Rev. Lett. **45**, 656 (1980).
¹²C. Y. Su, P. R. Skeath, I. Lindau, and W. E. Spicer, Surf. Sci. (in press).
¹³I. Hino, W. Petro, S. Eglash, W. E. Spicer, and I. Lindau (unpublished).
¹⁴C. Y. Su, I. Lindau, P. W. Chye, S.-J. Oh, and W. E. Spicer (unpublished).
¹⁵G. Lucovsky and R. S. Bauer, Solid State Commun. **31**, 931 (1979).
¹⁶W. A. Harrison, *Electronic Structure and the Properties of Solids* (Freeman, San Francisco, 1980), Chap. 11 and the solid-state table.
¹⁷C. Y. Su, P. R. Skeath, I. Hino, I. Lindau, and W. E. Spicer, Surf. Sci. (in press).
¹⁸C. D. Thuault, G. M. Guichar, and C. A. Sebenne, Surf. Sci. **80**, 273 (1979).
¹⁹See, for example, S. P. Singh-Boparai, M. Bowker, and

- D. A. King, *Surf. Sci.* **53**, 55 (1975).
- ²⁰P. Mark and W. F. Creighton, *Thin Solid Films* **56**, 19 (1979); P. Mark, S. C. Chang, W. F. Creighton, and B. W. Lee, *Crit. Rev. Solid State Sci.* **5**, 189 (1975).
- ²¹N. J. Shevchik, J. Tejada, and M. Cardona, *Phys. Rev. B* **9**, 2627 (1974).
- ²²D. Schmeisser and K. Jacobi, *Surf. Sci.* (in press).
- ²³S. A. Flodstrom, C. W. B. Martinsson, R. Z. Bachrach, S. B. M. Hagstrom, and R. S. Bauer, *Phys. Rev. Lett.* **40**, 907 (1978) and references cited.
- ²⁴C. M. Garner, C. Y. Su, W. E. Spicer, P. D. Elwood, D. Miller, and J. S. Harris, *Appl. Phys. Lett.* **34**, 934 (1979).
- ²⁵G. Lucovsky, *J. Vac. Sci. Technol.* **19**, 456 (1981).
- ²⁶O. Kubaschewski, *Metallurgical Thermochemistry*, 5th ed. (Oxford, New York, 1979).
- ²⁷Here we use the Knudsen-Hertz equation to calculate the evaporation rate, $R_{ev} = \alpha_v(p^* - p)/(2\pi mkT)^{1/2}$. In this equation α_v , the evaporation coefficient, is the fraction of evaporant flux that makes the transition from condensed to vapor phase; p^* is the vapor pressure of the evaporant; p is the hydrostatic pressure of

the return flux. With $\alpha_v = 10^{-7}$, $p^* = 1$ atm at $T = 643$ K, $p^* - p \approx p^*$, we obtain $R_{ev} = 7.5 \times 10^{15}$ mol/cm²sec. As stated in the text, 1 monolayer As₂O₃ can be evaporated in 0.1 sec. For the ~0.065 monolayer of chemically affected As atom to survive heating at 370 °C for 30 min, as is the case shown in Fig. 17, α_v has to be smaller than 3×10^{-11} . Such a small evaporation coefficient is not found to our knowledge. [L. I. Maissel and R. Glang, *Handbook of Thin Films* (McGraw-Hill, New York, 1970), Chap. 1.] In general, the evaporation coefficient is smaller when polymerization is involved in the vaporization process. For example, the evaporation coefficient of As has been measured to be 8.3×10^{-5} [M. B. Dowell, *J. Chem. Phys.* **66**, 1875 (1977)], where "polymerization" to As₂ and As₄ are required. For As₂O₃ in either the arsenolite or the claudetite form, units of As₄O₆ are clearly distinguishable, hence no polymerization is necessary when vaporized into As₄O₆ molecules. Therefore, we have no reason to expect the evaporation coefficient of As₂O₃ to be much lower than 10^{-4} .